European Centre
for Medium Range
Weather Forecasts

THE EFFECT OF REPLACING SOUTHERN HEMISPHERIC ANALYSES BY CLIMATOLOGY ON MEDIUM RANGE WEATHER FORECASTS

INTERNAL REPORT 2
RESEARCH DEPT.
JANUARY 1977

Centre Européen pour les Prévisions Météorologiques
a Moyen Terme

Europäisches Zentrum Für Mittelfristige Wettervorhersagen

THE EFFECT OF REPLACING SOUTHERN HEMISPHERIC ANALYSES BY CLIMATOLOGY ON MEDIUM RANGE WEATHER FORECASTS.

By

K. Arpe, J. Gibson and A. Hollingsworth
European Centre for Medium Range Weather Forecasts, Bracknell.

ECMWF
LIBRARY
No. 566
ECMWF
LIBRARY

A B S T R A C T

The effect of missing southern hemisphere observational data on medium range weather forecasts was studied numerically. By comparing a forecast based on actual analyses with one based on climatological fields on the southern hemisphere we found obvious differences in northern hemisphere mid latitudes after 7 days. However, both forecasts looked much more similar to each other than to observation and no forecast could be considered to be better or worse than the other.

This supports the conclusion by other authors that the southern hemisphere has little influence on northern hemisphere mid latitude forecasts for at least seven days.

1. Introduction

In carrying out medium range weather forecasts operationally it will sometimes happen that observational data will be missing for some days in certain regions. This is especially likely in the southern hemisphere due to unsatisfactory telecommunications. If data for the whole hemisphere is missing for some time objective analyses schemes will tend to produce climatological fields. In addition even with normal data availability, relatively few observations are received from the southern hemisphere, due to its sparse observational network. It is therefore of considerable interest to study the impact of such a loss of information on the forecasts.

BAUMHEFNER (1971,1972) and MIYAKODA and UMSCHEID (1973) found that the imposition of an equatorial "wall" will affect the forecasts at middle latitudes appreciably after 7 days and seriously after 12 days. DALEY (1974) showed with a barotropic model that the error in one hemisphere due to the imposition of a wall at the equator can largely be removed by a knowledge of the largest scales of the flow in the other hemisphere.

More experiments of this kind seem to be worth while because those few case studies are certainly not enough to draw final conclusions. Therefore we wanted to do a more realistic experiment by extending the experiment of MIYAKODA and UMSCHEID (1973) in the following way: We took the GFDL-N48-model instead of the GFDL-N24-model and we replaced the southern hemispheric analyses by climatological data instead of inserting a wall at the equator. The control run was based on global analyses by GFDL from 1 March 1965 00Z. A detailed description of the model and of this special case can be found at ARPE,BENGTSSON, HOLLINGSWORTH and JANJIC (1976), (later referred to as ABH&J).

2. Data Preparation

Two sources of data were used. One was analysed data from 1 March 1965 00Z, which was made available by GFDL. This dataset has been used for forecasting experiments by MIYAKODA et al (1970 ,1971,1974) and by ABH&J. The other dataset was climatological data for March for the southern hemisphere, which were made available by JENNE,CRUTCHER,VAN LOON and TALJAARD (1974). This provided fields of U,V,T(q) at five degreee intervals in latitude and longitude and at seven standard levels (SFC, 850, 700, 500, 300, 200, 100 mb).

2.1 Horizontal Interpolation

In the horizontal, linear interpolation was applied to the climatological data in two stages. First, data along lines of latitude were interpolated to mid point positions, and the Northern and Southern Latitude circles adjusted to 86.25°N and 86.25°S respectively, to conform with the requirements of a standard conversion routine. Secondly, a GFDL supplied routine was used to interpolate this data to the N48 modified Kurihara grid.

2.2 Vertical Interpolation

Vertical interpolation to sigma surfaces was performed using linear interpolation in log (pressure) . The values of p appropriate for each point were calculated from the relationship.

$$\sigma = \frac{p}{p*}$$, where p* is the surface pressure.

Since climatological data was available to 100 mb only, no attempt was made to extrapolate to the highest levels of the GFDL data. When the climatological data was extrapolated beyond 100 mb the fields derived were unrealistic so we used instead the analysed data for $\sigma = 0.0089$ and .074 which was the only southern hemisphere data available to us. We cannot determine the effect of this on our results at present.

2.3 Merging the Data

From the equator Northwards, the GFDL data was unchanged. To achieve a smooth transition to the climatological data, the data for the nine lines immediately South of the equator, (i.e. 0.89°-17.05°S) were derived according to the scheme

$$\frac{N}{10} A_{CLIMATE} + \frac{10-N}{10} A_{GFDL},$$

where A is u,v,T or q and N is number of lines South of the equator. From the tenth line South of the equator to the southernmost line climatological data was used.

This process was applied to the 7 lowest levels of U, V, and T, and to the 5 lowest levels of humidity variables.

By a mistake the interpolation was not done for the surface pressure p* and the surface pressure of the GFDL-analysis was taken instead. But according to the results of SMAGORINSKY, MIYAKODA and STRICKLER (1970) this will have reduced the effect on the forecast because the surface pressure in the GFDL model only represents a thickness of 9 mb.

To give an impression of the difference in the initial data Fig. 1 shows the initial 500 mb height field of the southern hemisphere for both forecasts.

3. Results

Unfortunately all data of the forecast with climatology were lost for the first 4-5 days of the ten day forecast. For convenience it was therefore assumed that both data sets had no significant differences in the mid latitudes of the Northern hemisphere before that date. In the figures the results of the forecast from the global analyses will be referred to as "N48-run" and those from the northern hemispheric analyses combined with climate data for the southern hemisphere will be referred to as "CLI-run". Only brief comparisons between the forecasts and the verifying analyses will be given because that has been done already by ABH&J (1976) and only differences in the two forecasts will be noted. The area for comparison and verification will be the troposphere (1000 mb - 200 mb) north of 20°N. This area was chosen because it is the largest area covered by observed data and the verifications of the control run, already referred to, were performed over the same region.

3.1 Comparison between the two forecasts

To compare the forecasts with each other Fig. 2 shows the root-mean-square (RMS) difference of geopotential height for the troposphere north of 20°N. To give a guideline the RMS difference between persistence and N48-run is included. (The definitions of RMS difference, correlation coefficient etc. may be found in ABH&J (1976)). The RMS differences of zonal means have a very fluctuating behaviour. As this will be evident more clearly later we will deal with it then. The waves with wave numbers 4 to 9 and 10 to 20 indicate a remarkable increase of discrepancies between the two forecasts after the 6th day.

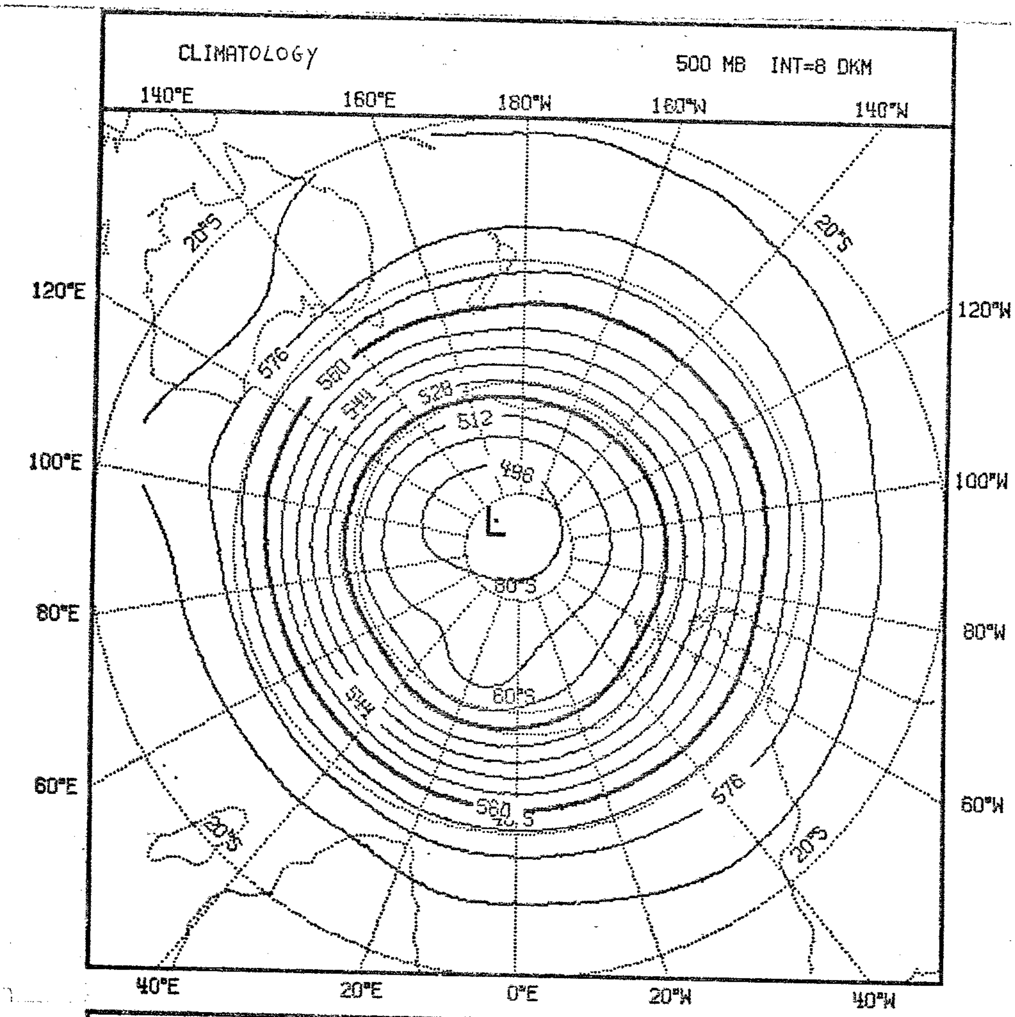
CLIMATOLOGY
500 MB INT=8 DKM
140°E
160°E
180°W
160°W
140°W
120°E
100°E
80°E
60°E
120°W
100°W
80°W
60°W
40°E
20°E
0°E
20°W
40°W
20°S
576
560
544
528
512
496
L
80°S
60°S
40°S

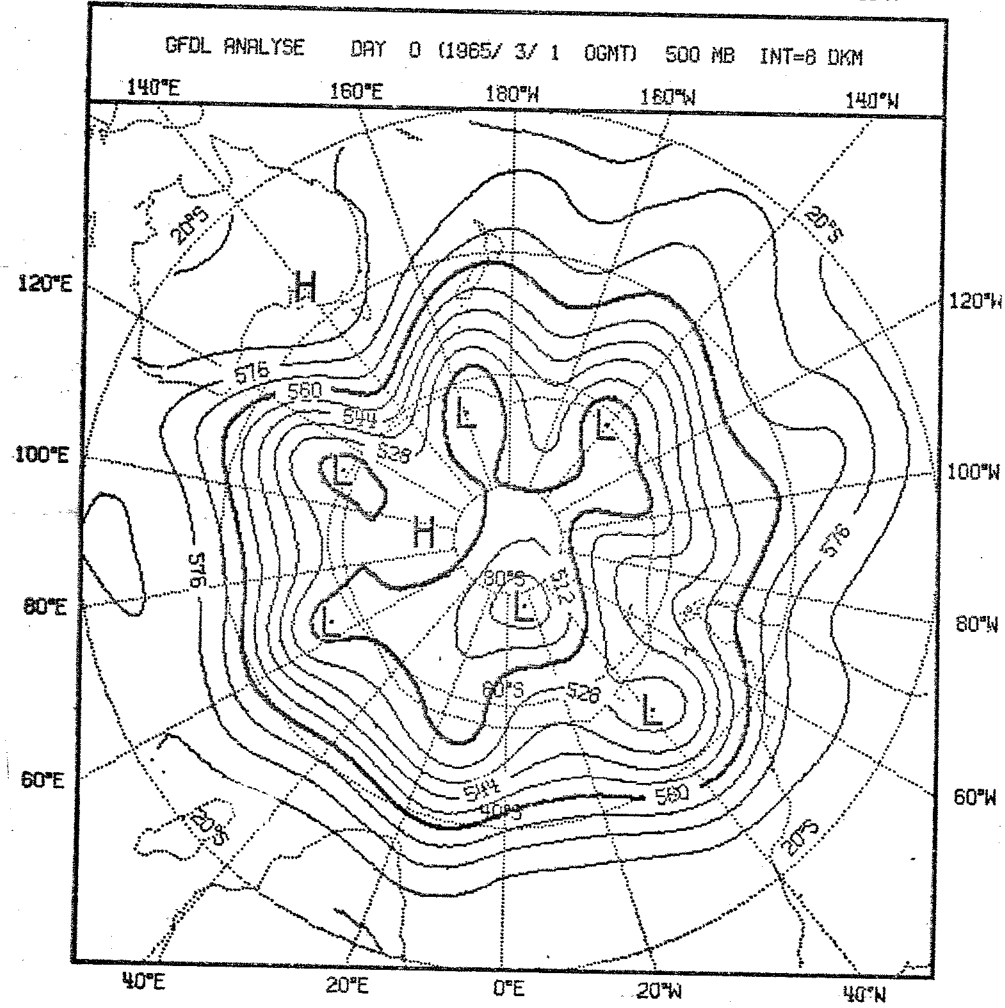
GFDL ANALYSE DAY 0 (1965/ 3/ 1 0GMT) 500 MB INT=8 DKM
140°E
160°E
180°W
160°W
140°W
120°E
100°E
80°E
60°E
120°W
100°W
80°W
60°W
40°E
20°E
0°E
20°W
40°W
20°S
576
560
544
528
512
H
L
80°S
60°S
40°S

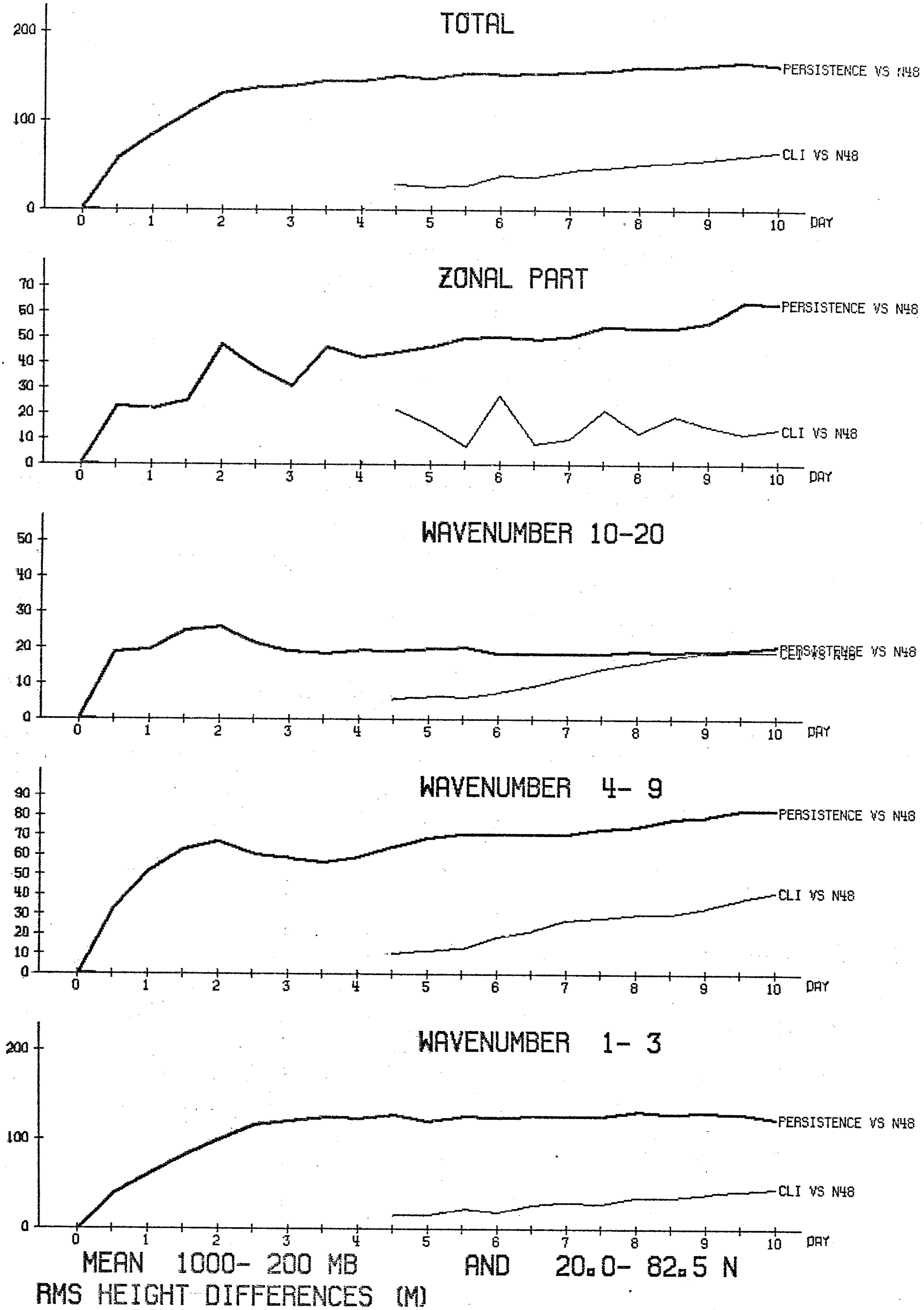
TOTAL
PERSISTENCE VS N48
CLI VS N48
DAY
ZONAL PART
PERSISTENCE VS N48
CLI VS N48
DAY
WAVENUMBER 10-20
PERSISTENCE VS N48
CLI VS N48
DAY
WAVENUMBER 4- 9
PERSISTENCE VS N48
CLI VS N48
DAY
WAVENUMBER 1- 3
PERSISTENCE VS N48
CLI VS N48
DAY
MEAN 1000- 200 MB AND 20.0- 82.5 N
RMS HEIGHT DIFFERENCES (M)

FIGURE 2

The latitudinal variation of the RMS difference is shown in Fig. 3. It might be expected that the difference would grow from the equator but this cannot be seen in the figure. It is rather the mid latitudes with their higher variances which have the greatest discrepancies. The experiment by MIYAKODA and UMSCHEID (1973) showed that the propagation of discrepancies from the equator could only be seen during the first four days with small amplitudes. This period is unfortunately not covered by Fig. 3. After that also in their experiment the maximum growth of discrepancies is found in mid latitudes. In a pressure-time-cross-section (Fig.4) it is indicated that these discrepancies are mainly growing in the higher troposphere where we find higher variances. This is in accordance with the results by MIYAKODA and UMSCHEID (1973). A growth of discrepancies from the bottom can be found too.

The RMS difference of the zonal means shows a strong oscillation with time for the whole troposphere. The fact that there is almost no vertical structure indicates that the mean surface pressure is causing this effect. In Fig. 5 a time sequence of the area-mean surface pressure for the northern hemisphere is plotted for both runs. Oscillations with amplitudes of about 1 mb and periods of about 0.8 days can be seen. These oscillations in surface pressure are due to axisymmetric external gravity wave modes arising from an initial imbalance of the mass fields in the two hemispheres. Because of the length of their period and the very large horizontal scale the Euler backward time differencing in the first twelve hours has little effect. The main difference between both runs is a phase difference of half a wavelength and the fact that in the CLI-run two modes of oscillation are obvious.

The correlation coefficients between the two forecasts shown in Fig. 6 are high except for the short waves (with wave number 10-20) after the 6th day. Then the correlation of these waves starts to decrease rapidly, reaching zero at the 10th day.

Fig. 7 shows the latitudinal variation of the correlation coefficients. It is interesting to note that the discrepancies (i.e. minimum correlations) not only grow from the equator, as might be expected, but also from the northpole, especially those of the waves with wave number 4 to 9. This is in contradiction to Fig. 3, which can easily be explained by the normalizing effect of the correlation coefficients.

It is surprising that we find at all wave number groups an early decrease of correlation north of 80°N although it is not found in the diagram for the total fields. It is probably not meaningful to compare zonal wave numbers north of 80°N with those south of 60°N and therefore the growth of error from the northpole may not be in the data themselves but caused by the method of spectral decomposition. In the correlation coefficients for the total fields the oscillation caused by the zonal part is indicated but only slightly because the waves are dominant.

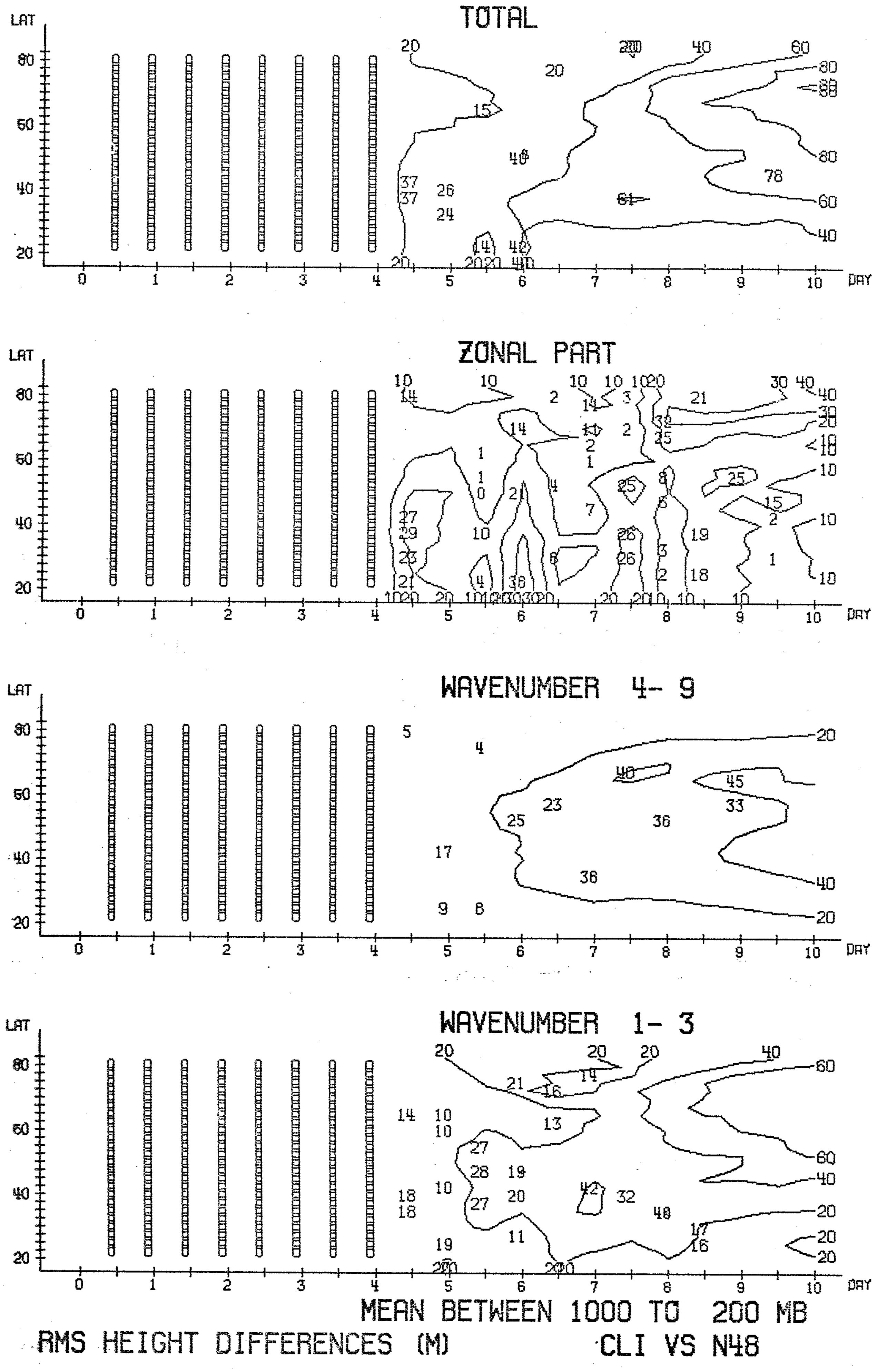
TOTAL
ZONAL PART
WAVENUMBER 4- 9
WAVENUMBER 1- 3
LAT
DAY
MEAN BETWEEN 1000 TO 200 MB
RMS HEIGHT DIFFERENCES (M)
CLI VS N48

FIGURE 3

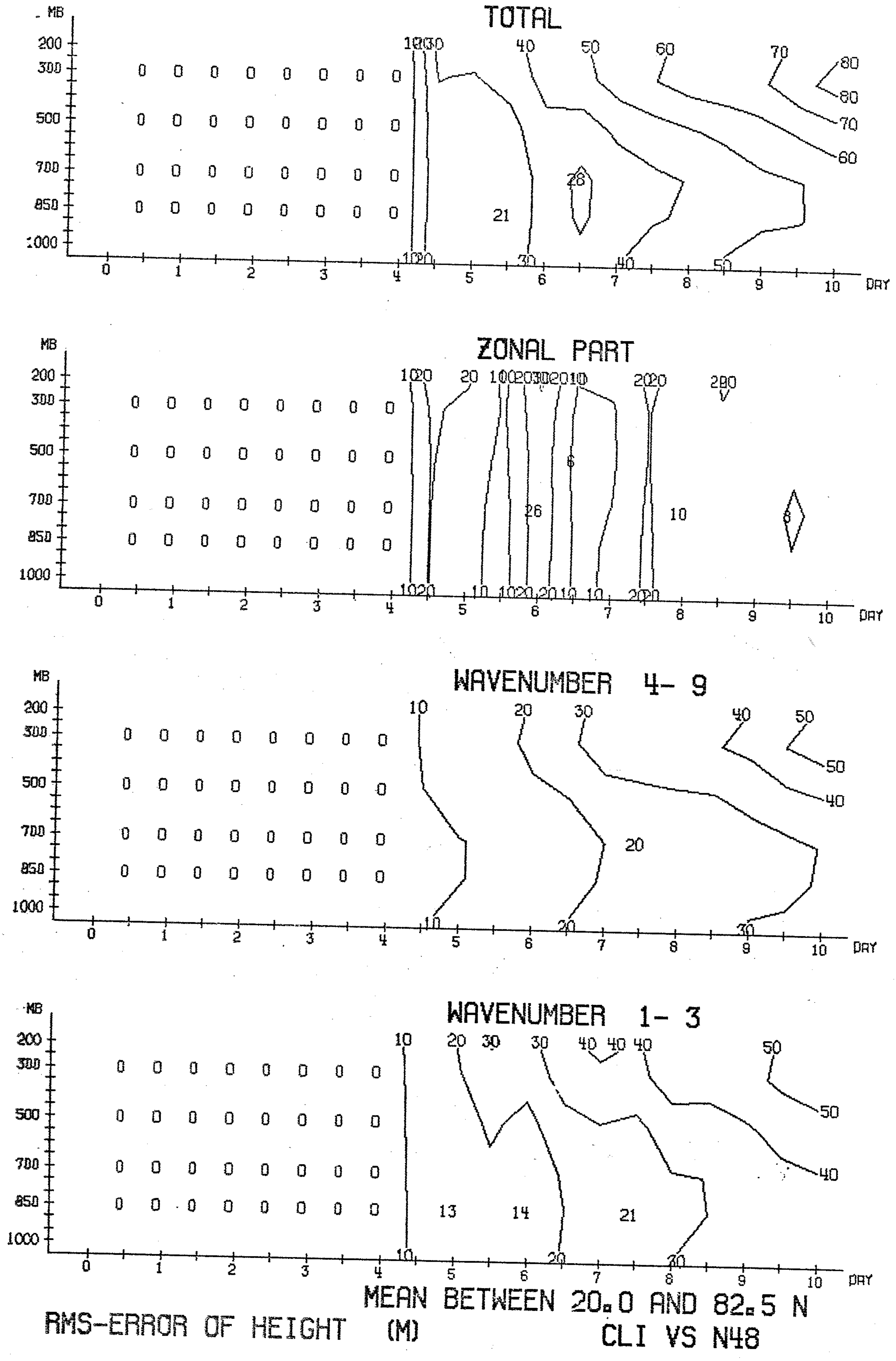
TOTAL
ZONAL PART
WAVENUMBER 4- 9
WAVENUMBER 1- 3
MB
200
300
500
700
850
1000
DAY
MEAN BETWEEN 20.0 AND 82.5 N
RMS-ERROR OF HEIGHT (M)
CLI VS N48

FIGURE 4

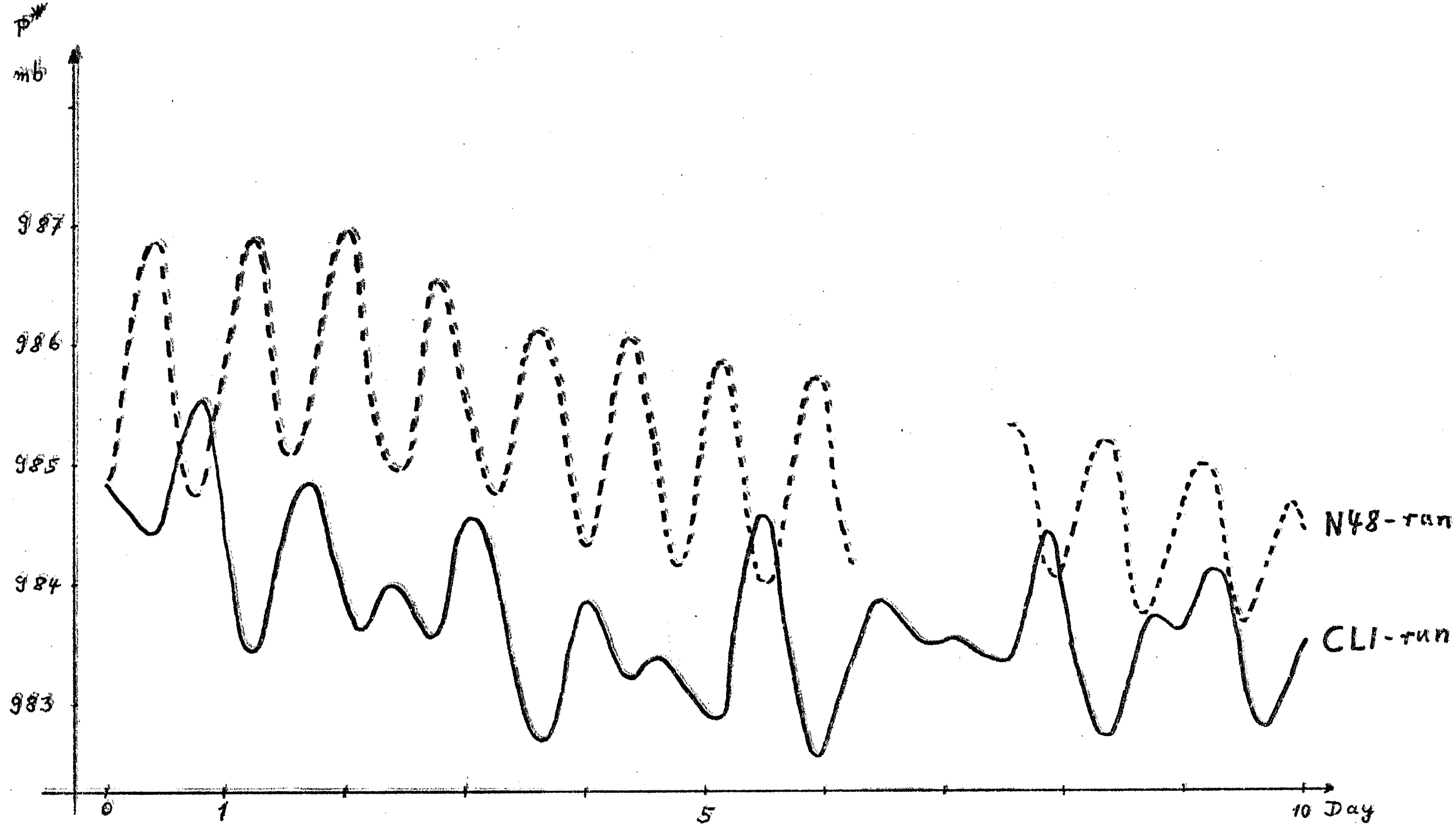

Fig. 5
Surface pressure p^*, average of the northern hemisphere
dashed line : N48-run
solid line : CLI-run

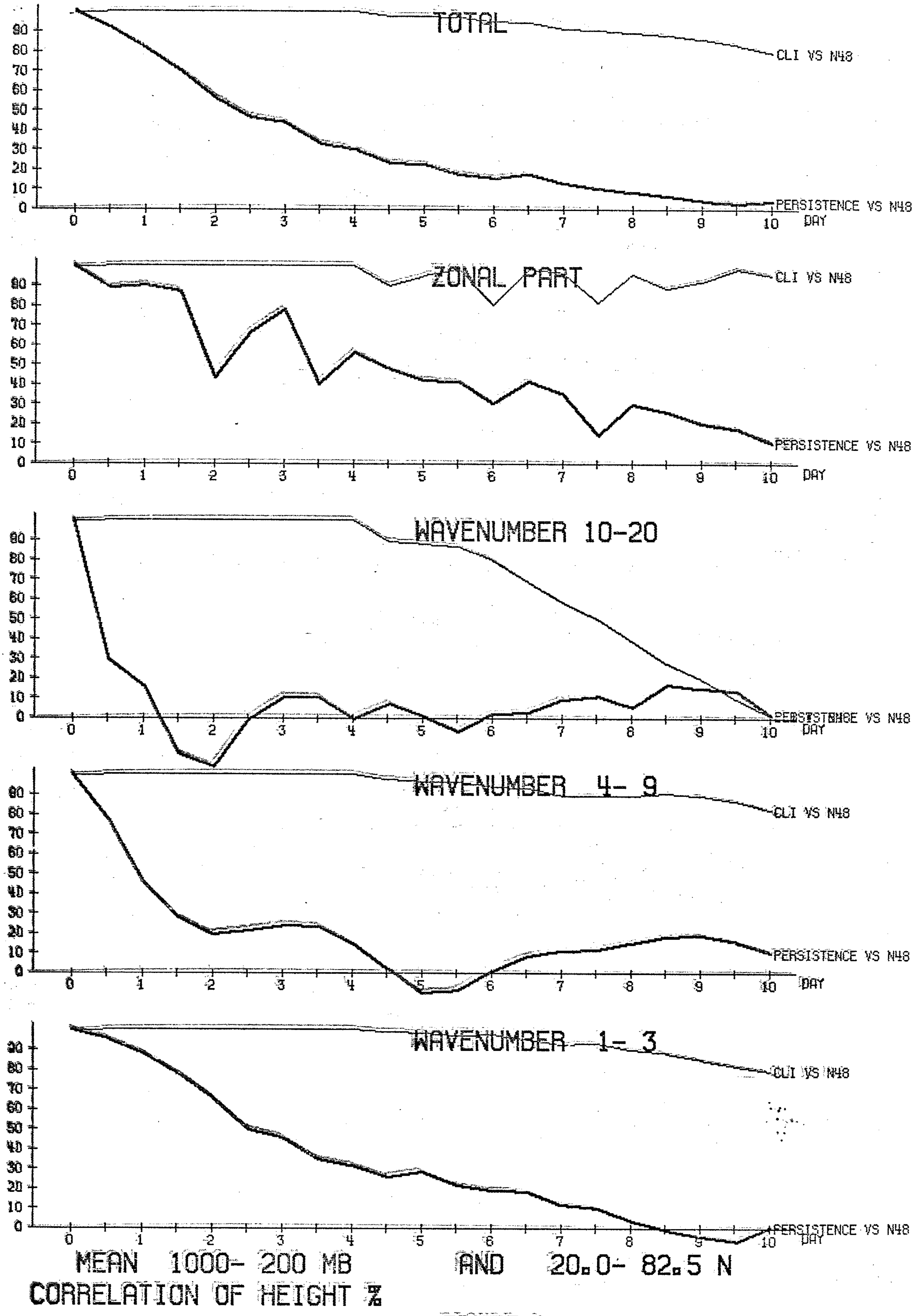
TOTAL
CLI VS N48
PERSISTENCE VS N48
DAY
ZONAL PART
CLI VS N48
PERSISTENCE VS N48
DAY
WAVENUMBER 10-20
PERSISTENCE VS N48
DAY
WAVENUMBER 4- 9
CLI VS N48
PERSISTENCE VS N48
DAY
WAVENUMBER 1- 3
CLI VS N48
PERSISTENCE VS N48
DAY
MEAN 1000- 200 MB AND 20.0- 82.5 N
CORRELATION OF HEIGHT %

FIGURE 6

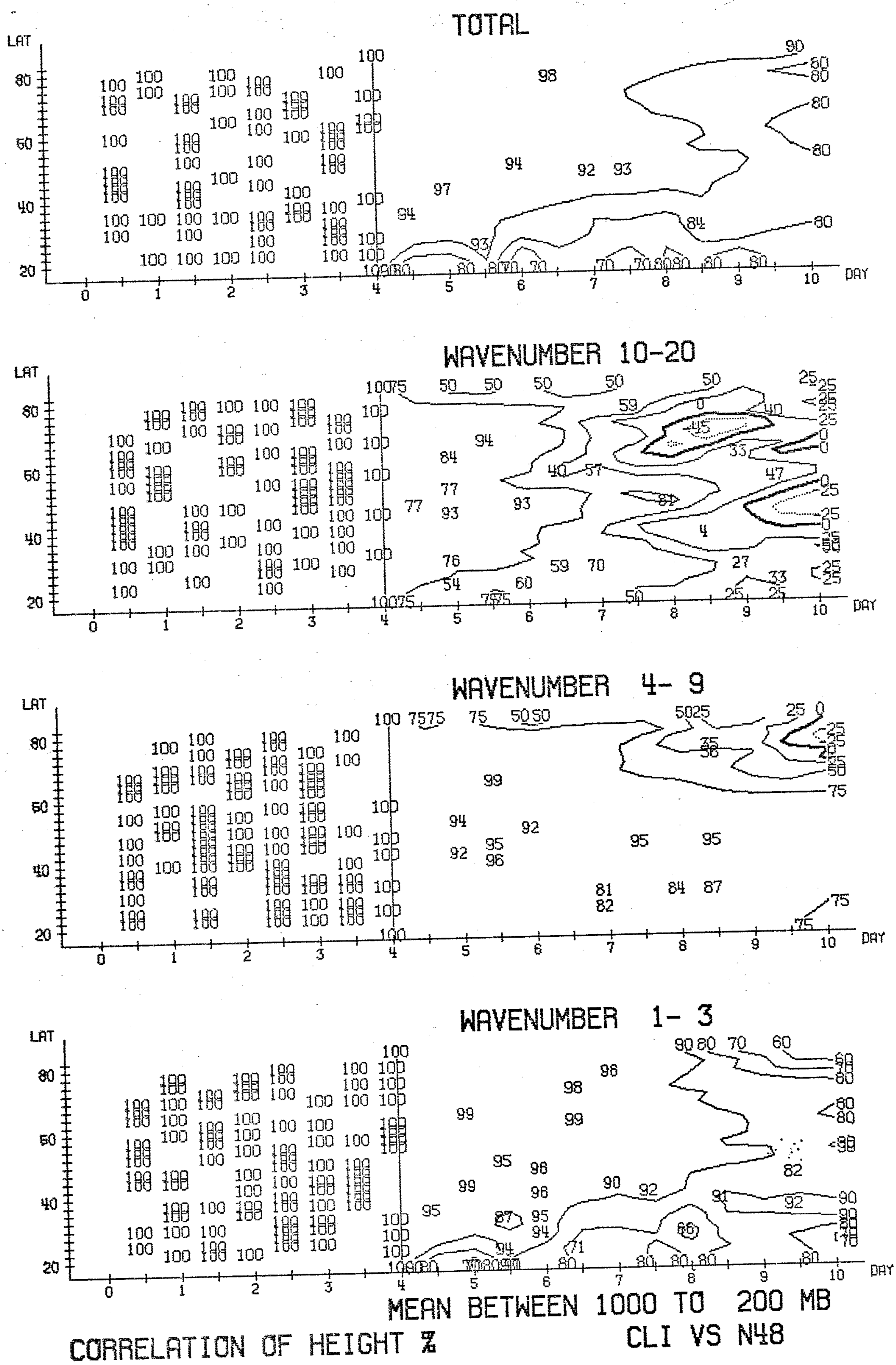
TOTAL
WAVENUMBER 10-20
WAVENUMBER 4- 9
WAVENUMBER 1- 3
LAT
DAY
MEAN BETWEEN 1000 TO 200 MB
CLI VS N48
CORRELATION OF HEIGHT %

FIGURE 7

The vertical distribution of the correlation coefficients in fig. 8 gives evidence that the lower troposphere is affected first by the different southern hemisphere initial data. The oscillation of the correlation coefficients of the zonal means has already been discussed above (see fig. 4).

3.2 Synoptic comparison

In the following a comparison of each forecast with the other and with the analyses will be carried out. Figures 9 to 12 give some examples to show the differences between the two forecasts. Each figure contains maps of both forecasts, a map of their discrepancies, and a map of the verifying NMC analysis. On the 500 mb height maps for the 5th day (fig. 9) both forecasts look very similar, only the two lows over the Pacific and over North America are somewhat deeper in the forecast with climate data. The difference map shows clearly that the CLI-run has lower values over almost the whole area except the Atlantic. This is probably connected with the oscillation of mean surface pressure of the northern hemisphere shown in fig. 5.

In fig. 10 the 500 mb height maps of the 7th day show an increase of discrepancies. The positions of the troughs over Greenland and over Europe are a little different but as they are so much more similar to each other than to the observed ones it can hardly be judged which forecast is better.

At the 9th day (fig. 11) the discrepancies between the two forecasts become even more pronounced. It can be said that the pattern of the CLI-run between 50°W and 90°W looks more like the observed pattern than that of the N48-run.

Figure 12 gives an example of 1000 mb height maps which does not give a clear-cut indication of an advantage for either of the forecasts.

The following figures will show the behaviour of troughs and ridges during the last five days by means of Hovmöller's trough-ridge-diagrams, but with a spectral decomposition. For easier comparison in each figure the axes of the troughs and ridges of the NMC analyses (lowest pictures) are copied on the upper pictures. In 500 mb at 70°N (fig.13) the CLI-run gives better positions of the long wave trough and ridge at 315°E and 240°E than the N48-run and the intensity at 240°E is better too. But further south at 40°N and 500 mb (fig.14) discrepancies between the two forecasts can hardly be seen for all days and a good agreement with observation is obvious. The forecasts of the long waves at 1000 mb are very similar to those of 500 mb and therefore not shown.

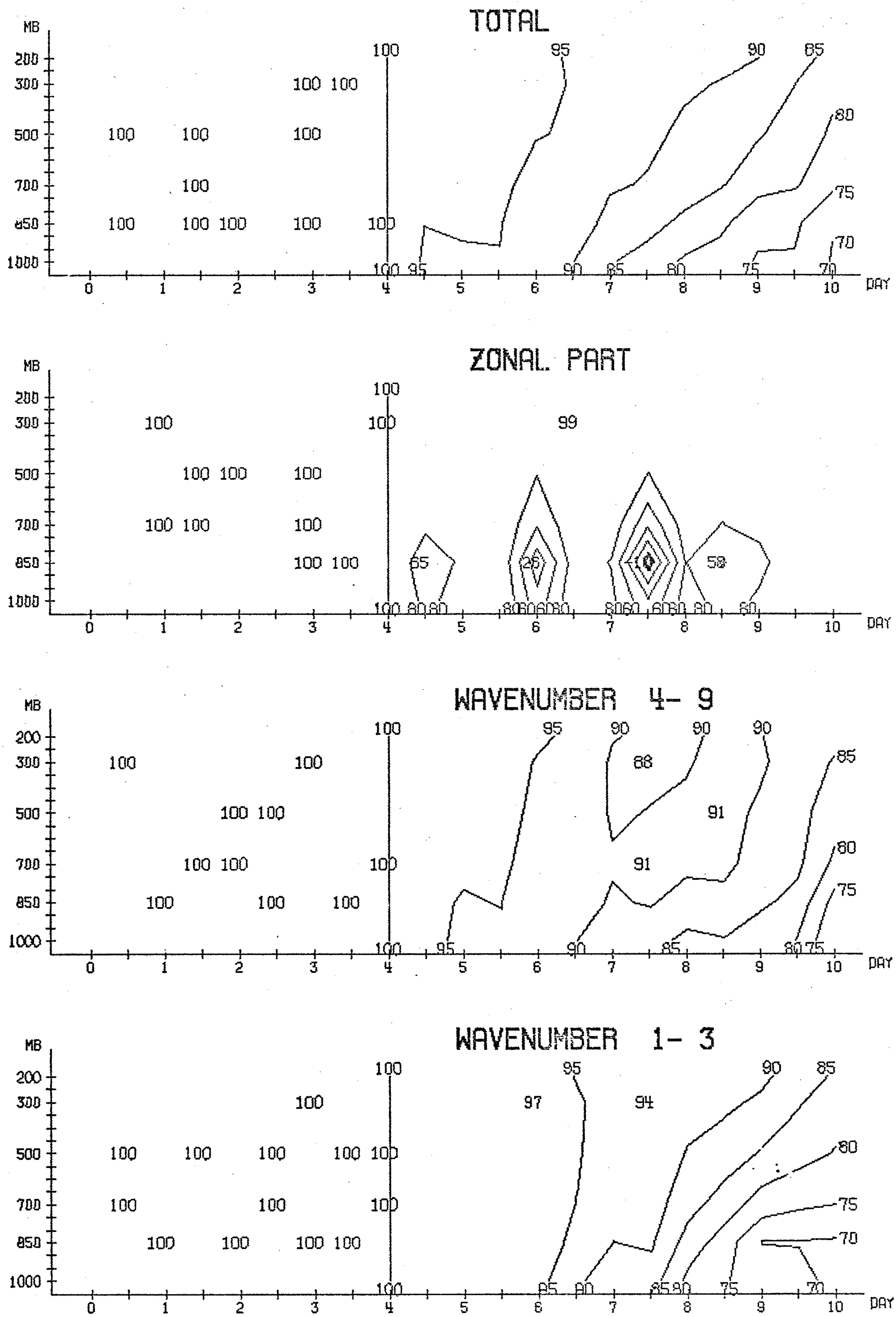

MEAN BETWEEN 20.0 AND 82.5 N

CORRELATION OF HEIGHT % CLI VS N48

FIGURE 8

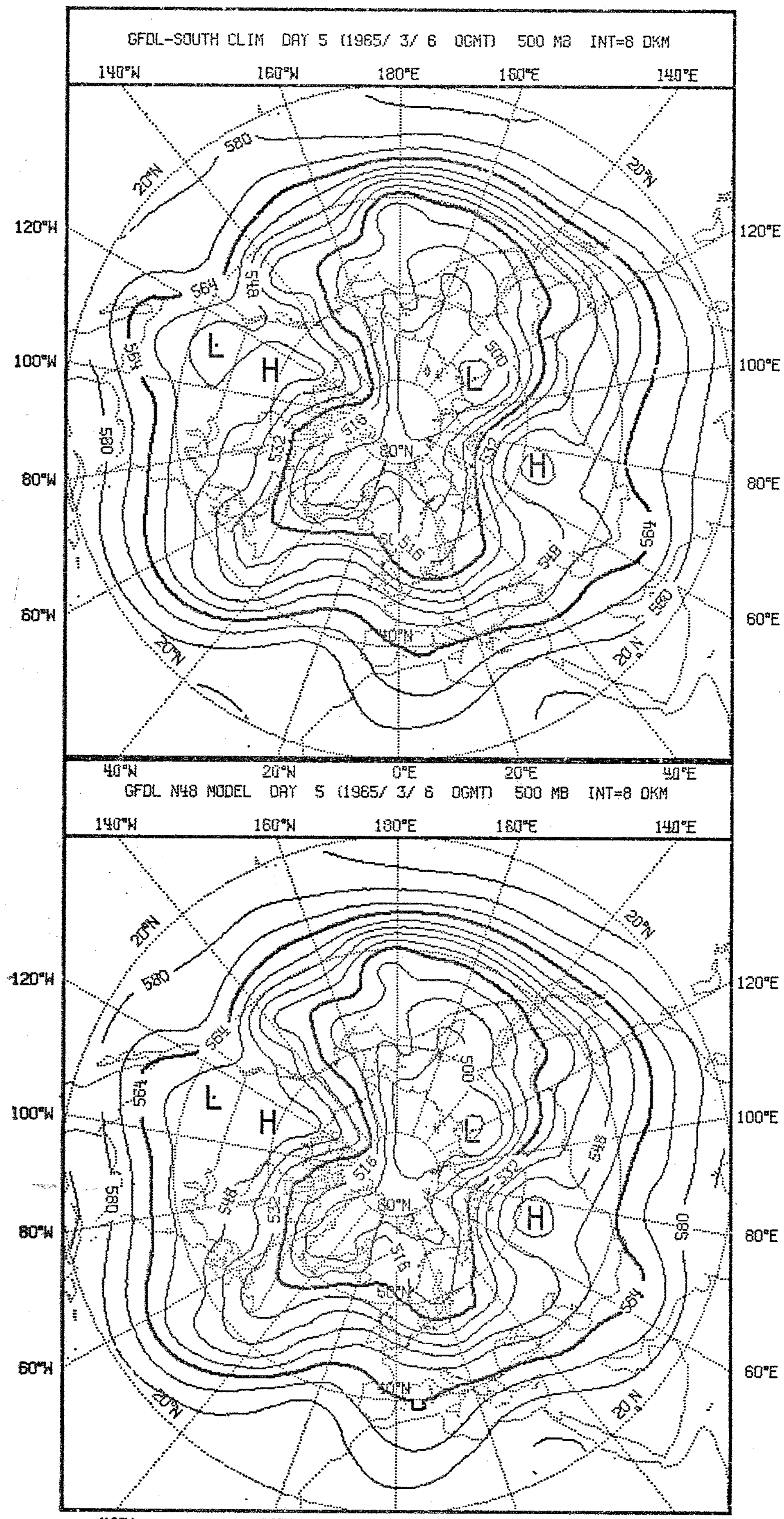
GFDL-SOUTH CLIM DAY 5 (1965/ 3/ 6 0GMT) 500 MB INT=8 DKM
140°W
160°W
180°E
160°E
140°E
120°W
120°E
100°W
100°E
80°W
80°E
60°W
60°E
40°W
20°W
0°E
20°E
40°E
GFDL N48 MODEL DAY 5 (1965/ 3/ 6 0GMT) 500 MB INT=8 DKM
140°W
160°W
180°E
160°E
140°E
120°W
120°E
100°W
100°E
80°W
80°E
60°W
60°E
40°W
20°W
0°E
20°E
40°E

FIGURE 9

NMC ANALYSIS DAY 7 (1965/ 3/ 8 0GMT) 500 MB INT=8 DKM

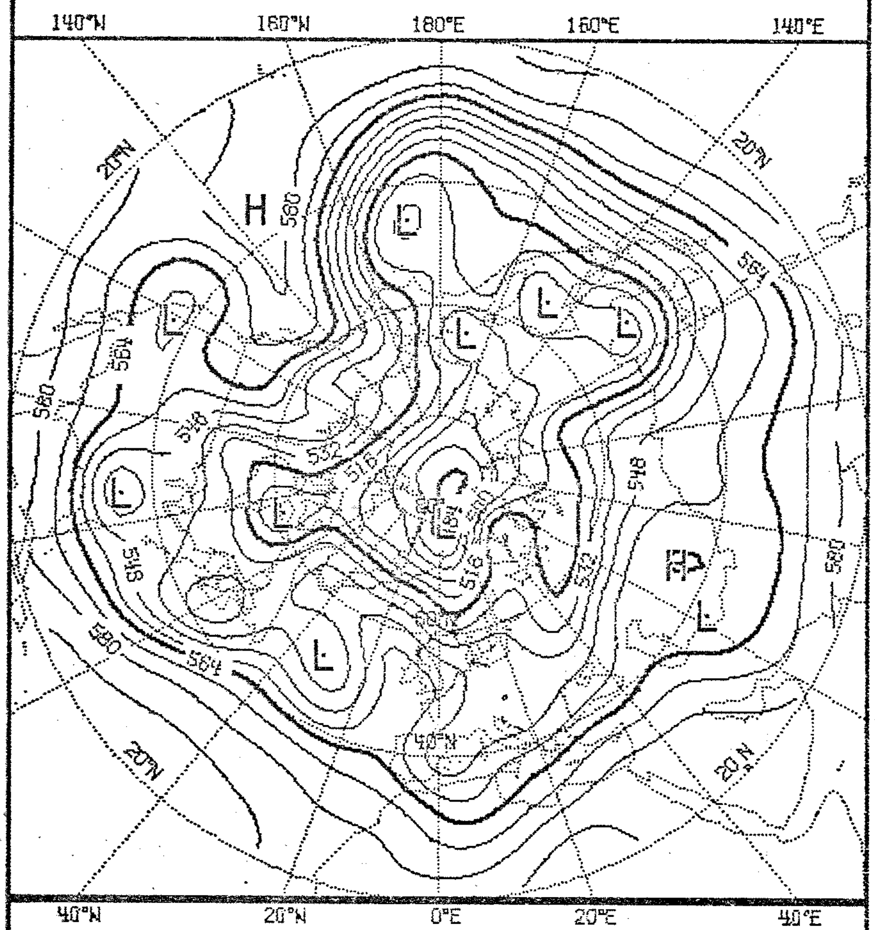

GFDL-SOUTH CLIM DIFFERENCE TO GFDL-N48 DAY 7 500 MB 8 DKM

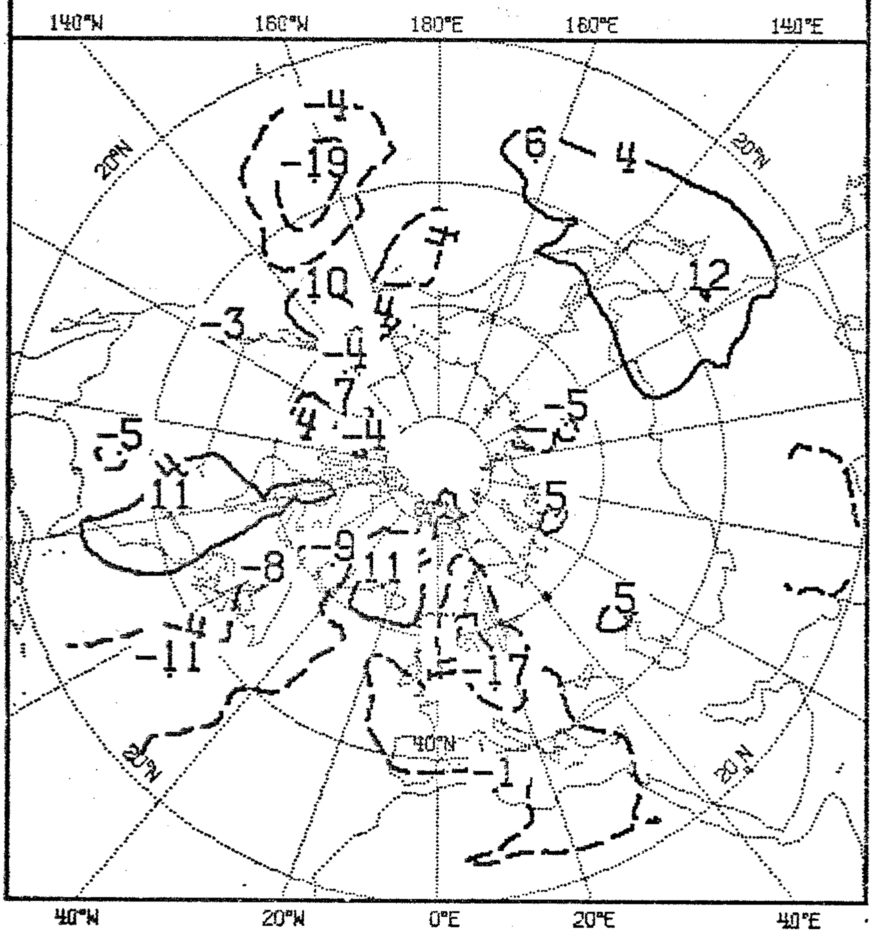

ECMWF LIBRARY

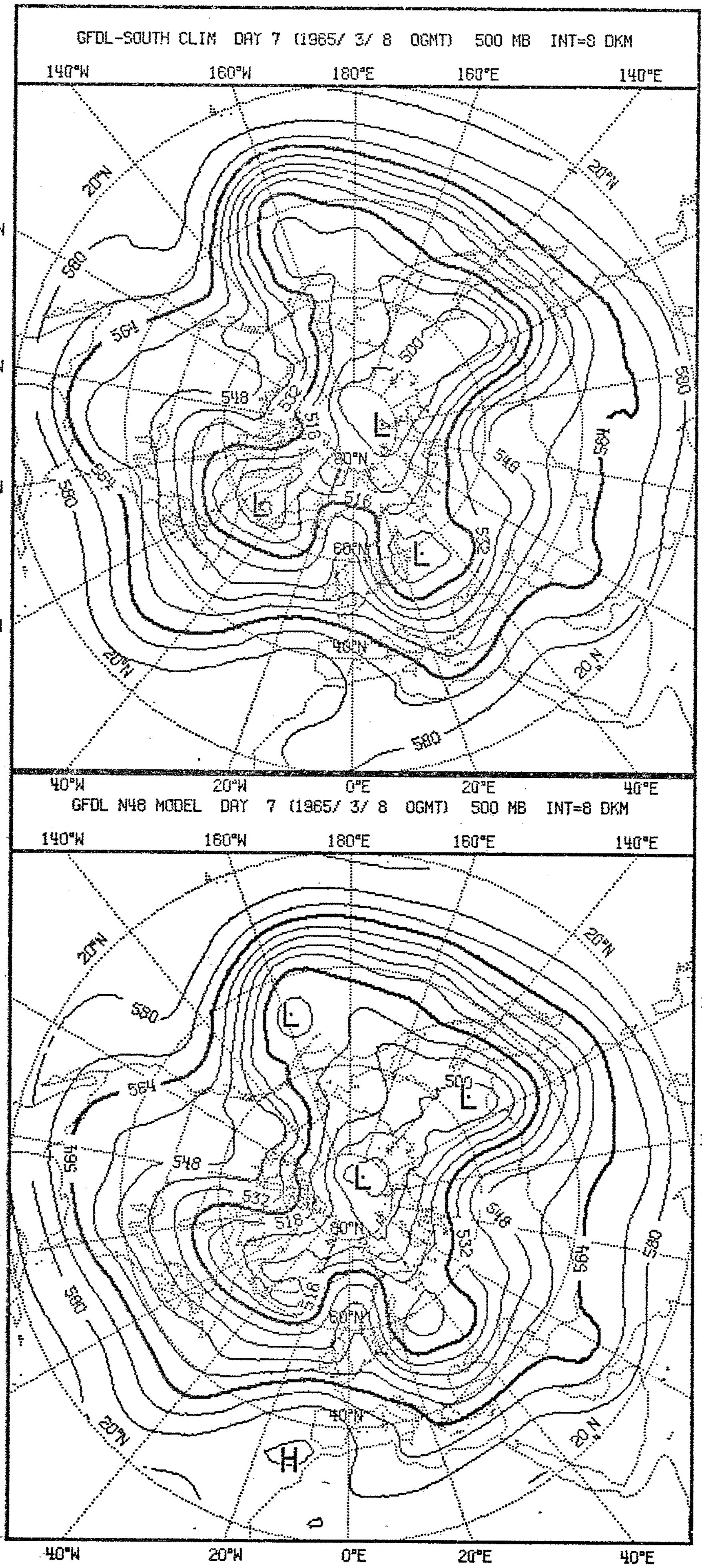
GFDL-SOUTH CLIM DAY 7 (1965/ 3/ 8 0GMT) 500 MB INT=8 DKM
140°W
160°W
180°E
160°E
140°E
120°W
100°W
80°W
60°W
120°E
100°E
80°E
60°E
40°W
20°W
0°E
20°E
40°E
GFDL N48 MODEL DAY 7 (1965/ 3/ 8 0GMT) 500 MB INT=8 DKM

FIGURE 10

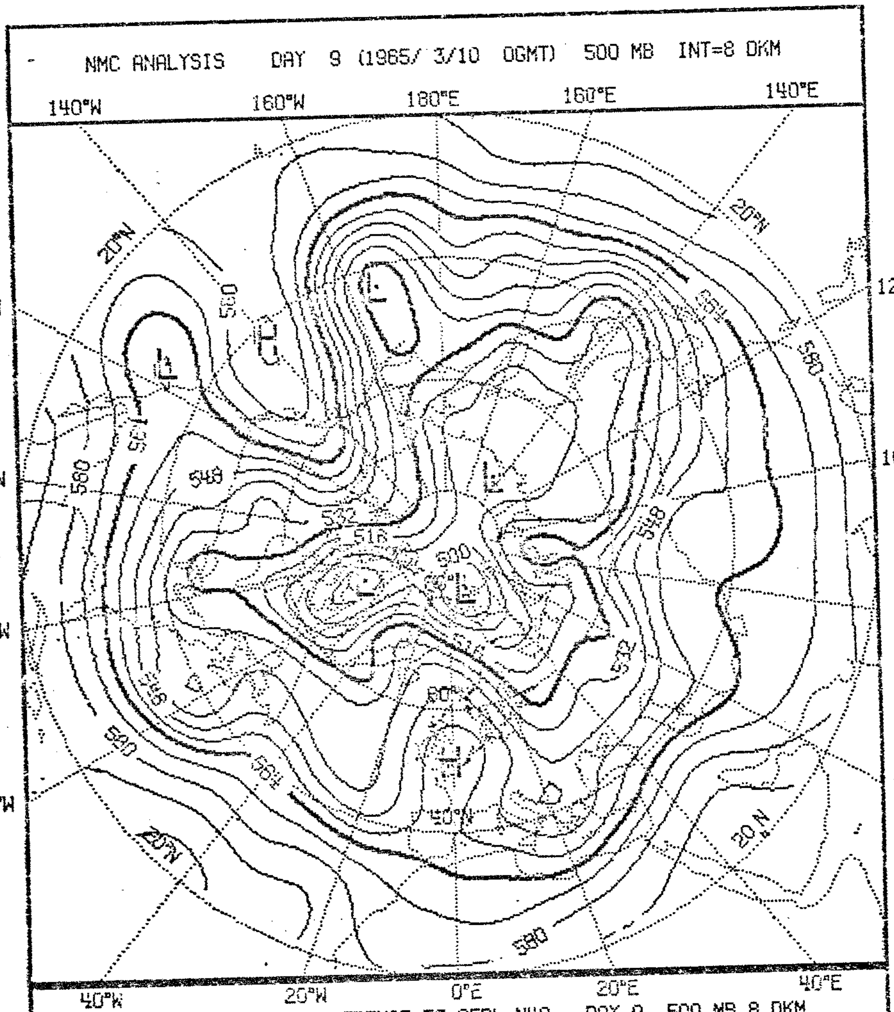

NMC ANALYSIS DAY 9 (1965/ 3/10 0GMT) 500 MB INT=8 DKM
140°W 160°W 180°E 160°E 140°E
120°W 120°E
100°W 100°E
80°W 80°E
60°W 60°E
40°W 20°W 0°E 20°E 40°E

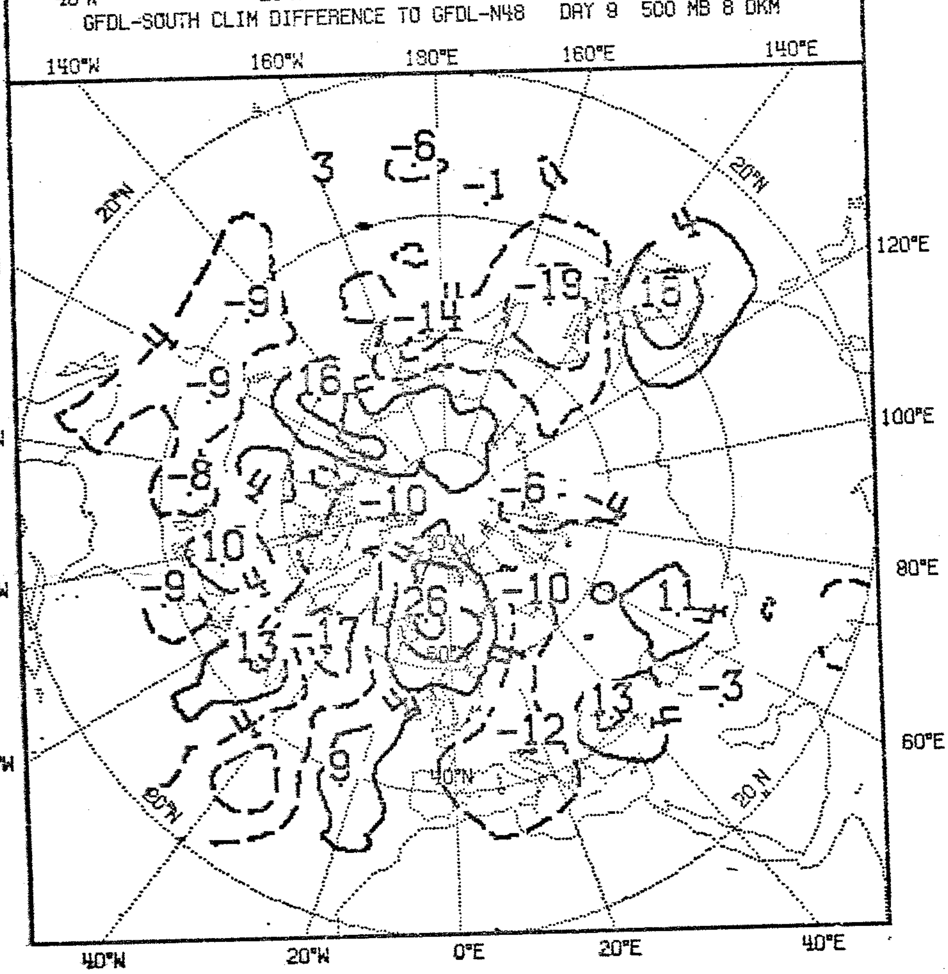

GFDL-SOUTH CLIM DIFFERENCE TO GFDL-N48 DAY 9 500 MB 8 DKM
140°W 160°W 180°E 160°E 140°E
120°W 120°E
100°W 100°E
80°W 80°E
60°W 60°E
40°W 20°W 0°E 20°E 40°E

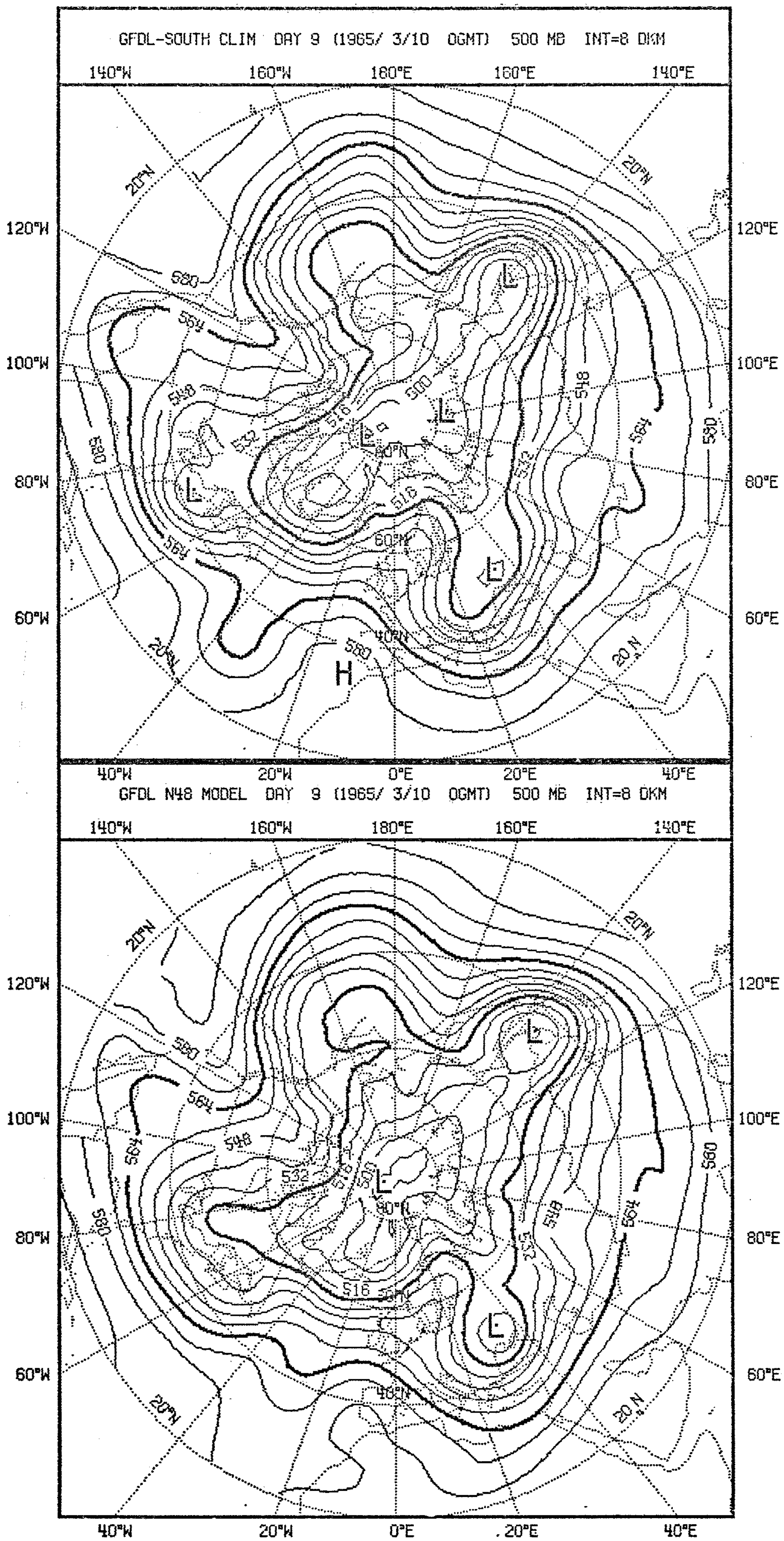
GFDL-SOUTH CLIM DAY 9 (1965/ 3/10 0GMT) 500 MB INT=8 DKM
140°W
160°W
180°E
160°E
140°E
120°W
100°W
80°W
60°W
120°E
100°E
80°E
60°E
40°W
20°W
0°E
20°E
40°E
GFDL N48 MODEL DAY 9 (1965/ 3/10 0GMT) 500 MB INT=8 DKM

FIGURE 11

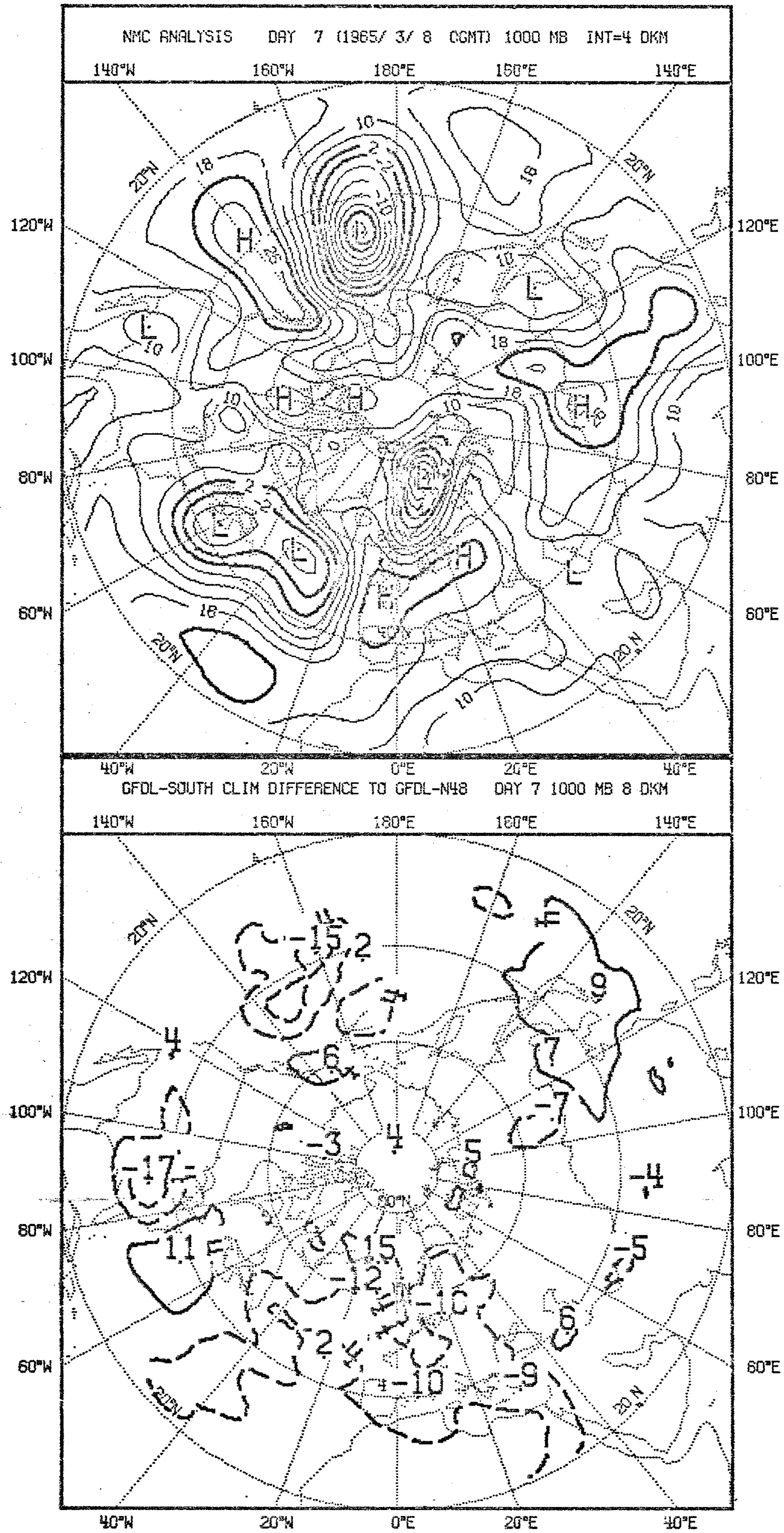
NMC ANALYSIS DAY 7 (1965/ 3/ 8 0GMT) 1000 MB INT=4 DKM
140°W
160°W
180°E
160°E
140°E
120°W
100°W
80°W
60°W
120°E
100°E
80°E
60°E
40°W
20°W
0°E
20°E
40°E
GFDL-SOUTH CLIM DIFFERENCE TO GFDL-N48 DAY 7 1000 MB 8 DKM

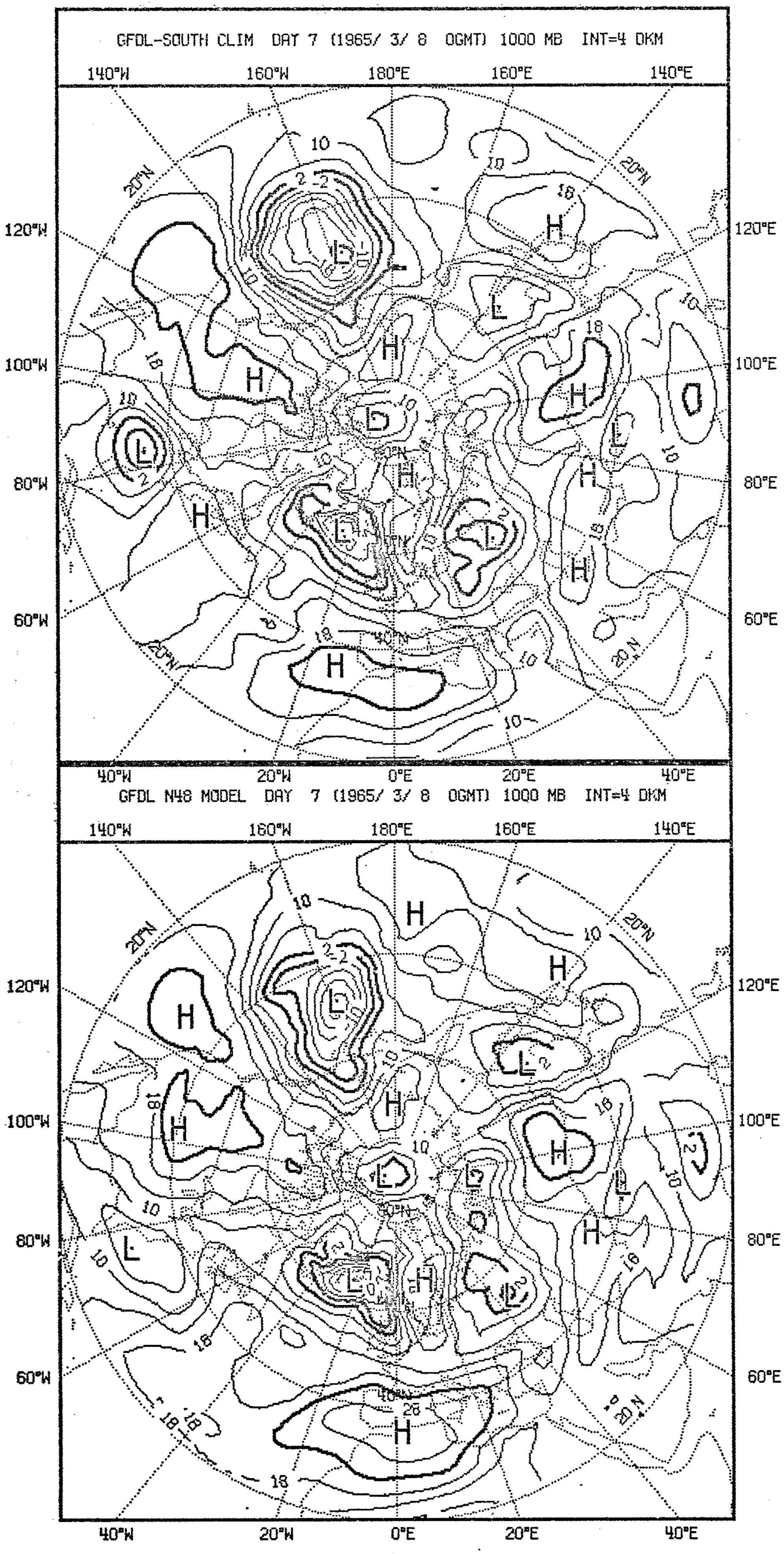
GFDL-SOUTH CLIM DAY 7 (1965/ 3/ 8 0GMT) 1000 MB INT=4 DKM
140°W
160°W
180°E
160°E
140°E
120°W
100°W
80°W
60°W
120°E
100°E
80°E
60°E
40°W
20°W
0°E
20°E
40°E
GFDL N48 MODEL DAY 7 (1965/ 3/ 8 0GMT) 1000 MB INT=4 DKM
140°W
160°W
180°E
160°E
140°E
120°W
100°W
80°W
60°W
120°E
100°E
80°E
60°E
40°W
20°W
0°E
20°E
40°E

FIGURE 12

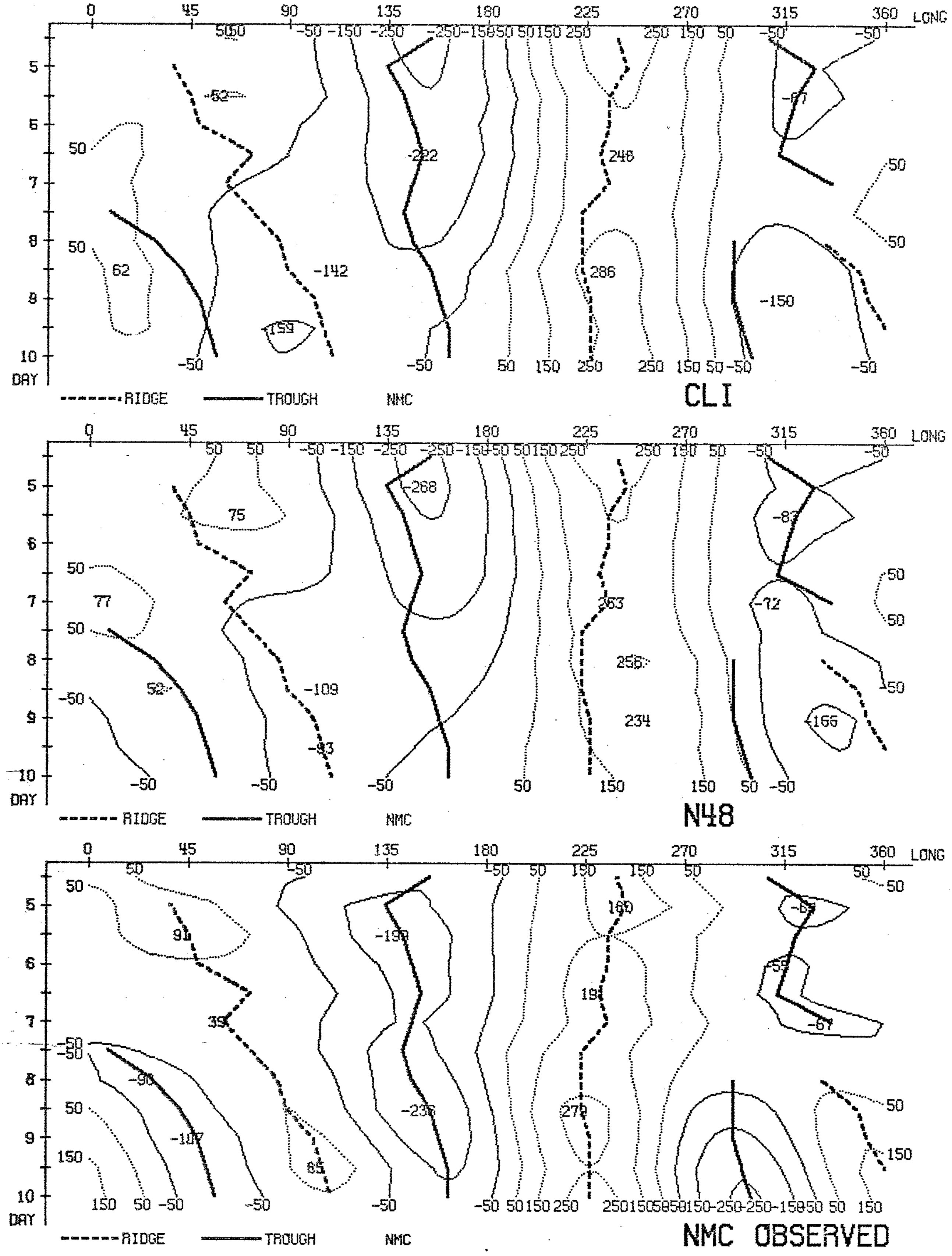

WAVENUMBER 1- 3 LATITUDE 70.0 N LEVEL 500 MB
GEOP. HEIGHT

FIGURE 13

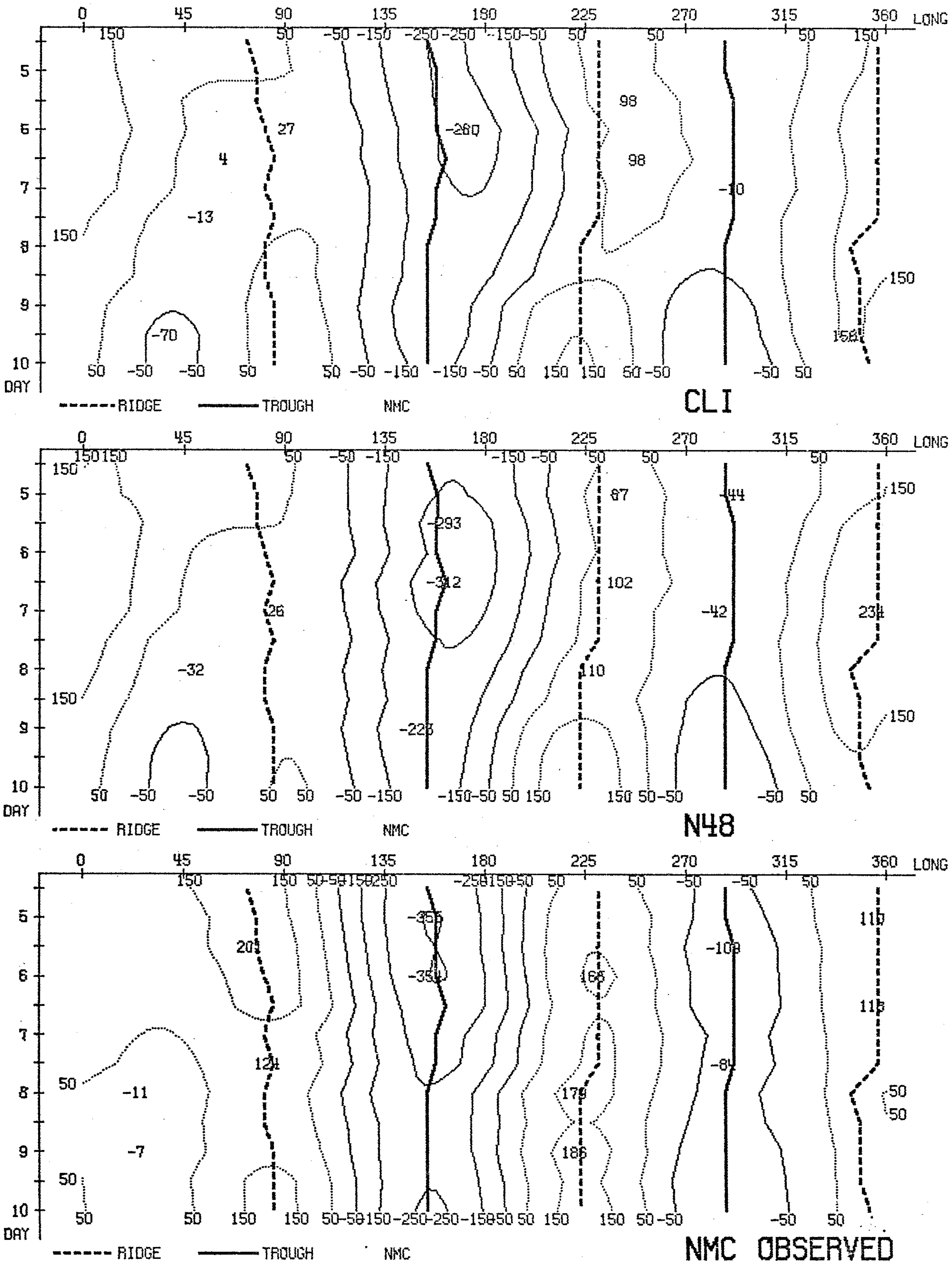

WAVENUMBER 1- 3 LATITUDE 40.0 N LEVEL 500 MB
GEOP. HEIGHT

FIGURE 14

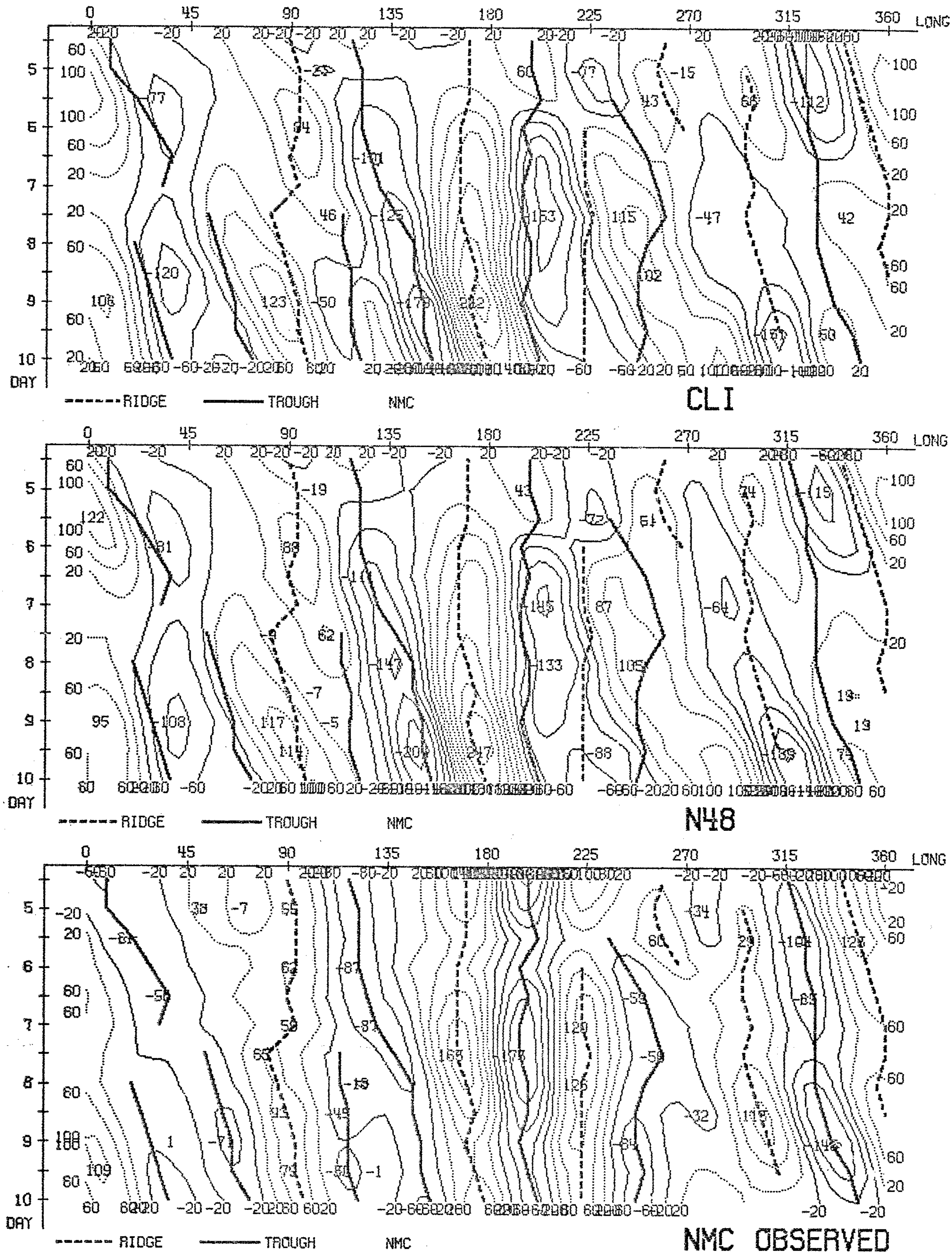

WAVENUMBER 4- 9 LATITUDE 50.0 N LEVEL1000 MB
GEOP. HEIGHT

FIGURE 15

In the diagrams for the medium wave length band (wave numbers 4 to 9) it can be seen (fig. 15) that both forecasts are much more similar to each other than to observation. The position of the strongest ridge at about 200°E is forecast well but the adjoining trough and ridge to the east have smaller wave length in the observed fields than in the forecast ones. As this region is just the Pacific one cannot be sure that the NMC-analyses are always right.

3.3 Conventional skill scores

To get an objective comparison between both forecasts and the analyses, the same skill scores will be used as already described by ABH&J (1976). Although it has been stated several times that the RMS-error is not very good for judging the quality of a forecast we start with it because most scientists are used to it and because an ideal skill score is not yet known. Fig. 16 gives a mean RMS-error for the height field of the troposphere north of 20°N. It has to be kept in mind that all data of the CLI-run were lost for the first 4 days and those of the N48-run were taken instead.

In fig. 16 the differences between the two forecasts are very small with a slight advantage for the N48-run until day 8½ and a slight advantage for the CLI-run thereafter. The same results hold when the data are smoothed in time before comparing them (fig. 17). The main difference between fig. 16 and 17 is that the RMS-error is somewhat smaller, especially for short waves. The latitudinal and vertical variation of the RMS-error of the long waves is very similar for both forecasts and therefore not shown.

More variation with latitude of the RMS-error can be seen for the zonal means (fig. 18). A time smoothing of the data was chosen because of its smoother pattern. At about 35°N the CLI-run shows a slight advantage and at about 55°N the N48-run has less values.

A first overview of the correlation coefficients in fig. 19 shows that it is only worth looking into more detail for the long waves because the correlation of the other waves is already down to almost zero by 4½ days, when data of the CLI-run become available. Again it can be seen that the differences between the two forecasts are very small. The latitude-time cross-sections for the long waves(fig.20) show different skill at 30°N and about 60°N. The height field of the northern latitudes was forecast better by the CLI-run and that of the southern latitudes by the other one.

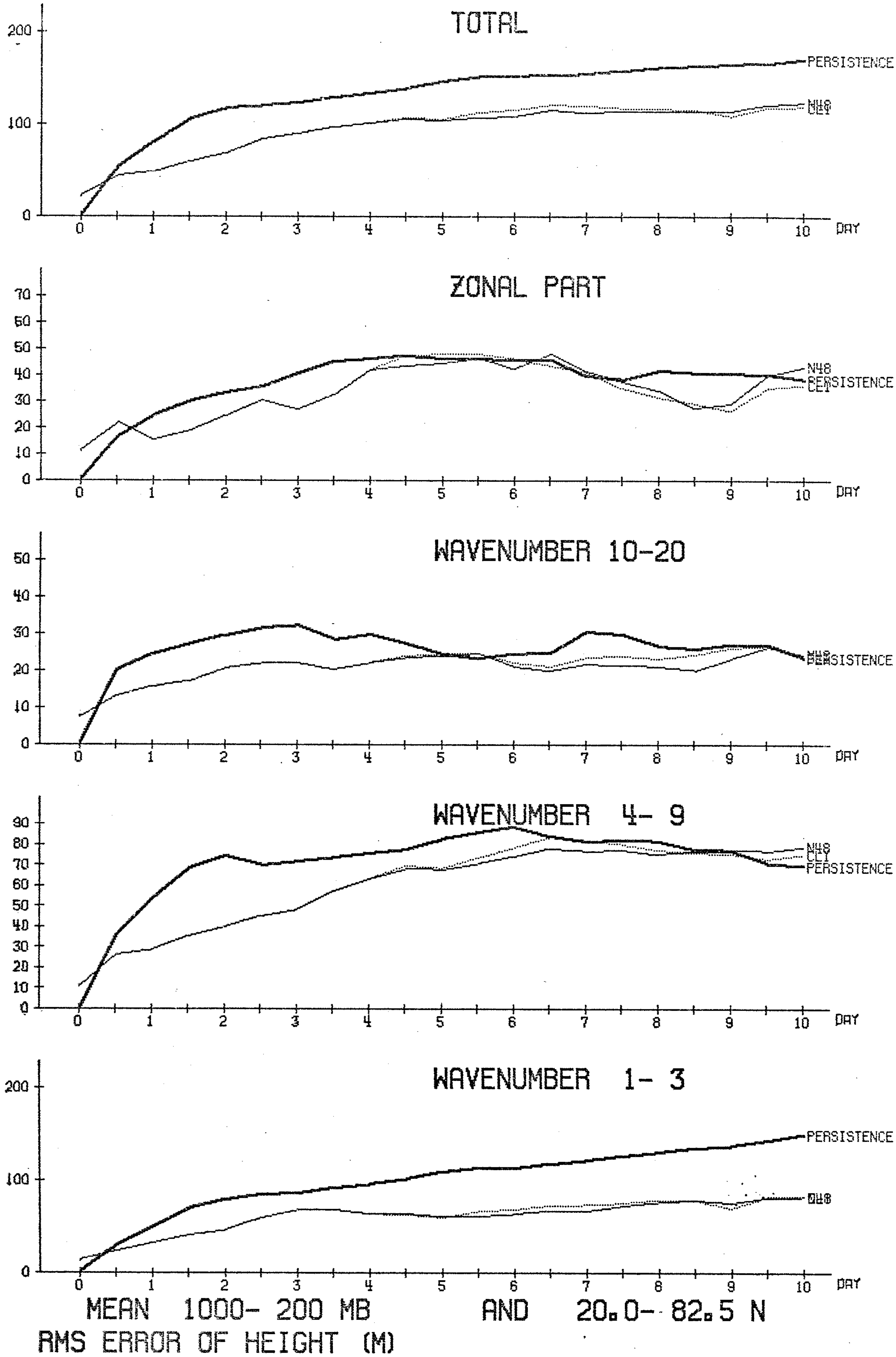

TOTAL
PERSISTENCE
N48
CLT
ZONAL PART
N48
PERSISTENCE
CLT
WAVENUMBER 10-20
N48
PERSISTENCE
WAVENUMBER 4- 9
N48
CLT
PERSISTENCE
WAVENUMBER 1- 3
PERSISTENCE
N48
DAY
MEAN 1000- 200 MB AND 20.0- 82.5 N
RMS ERROR OF HEIGHT (M)

FIGURE 16

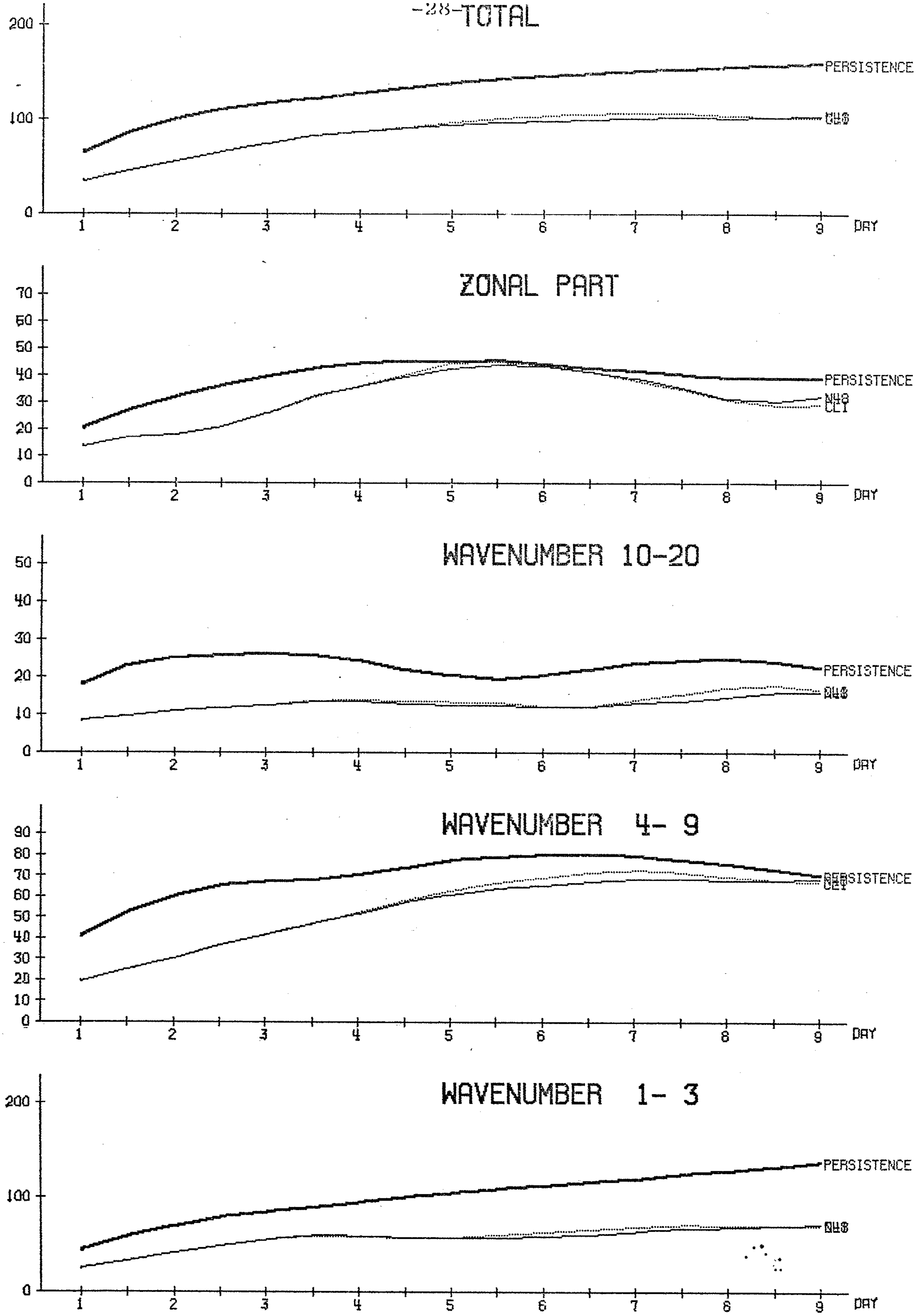

MEAN 1000- 200 MB AND 20.0- 82.5 N

RMS ERROR OF HEIGHT (M) 60 HOUR MEAN

FIGURE 17

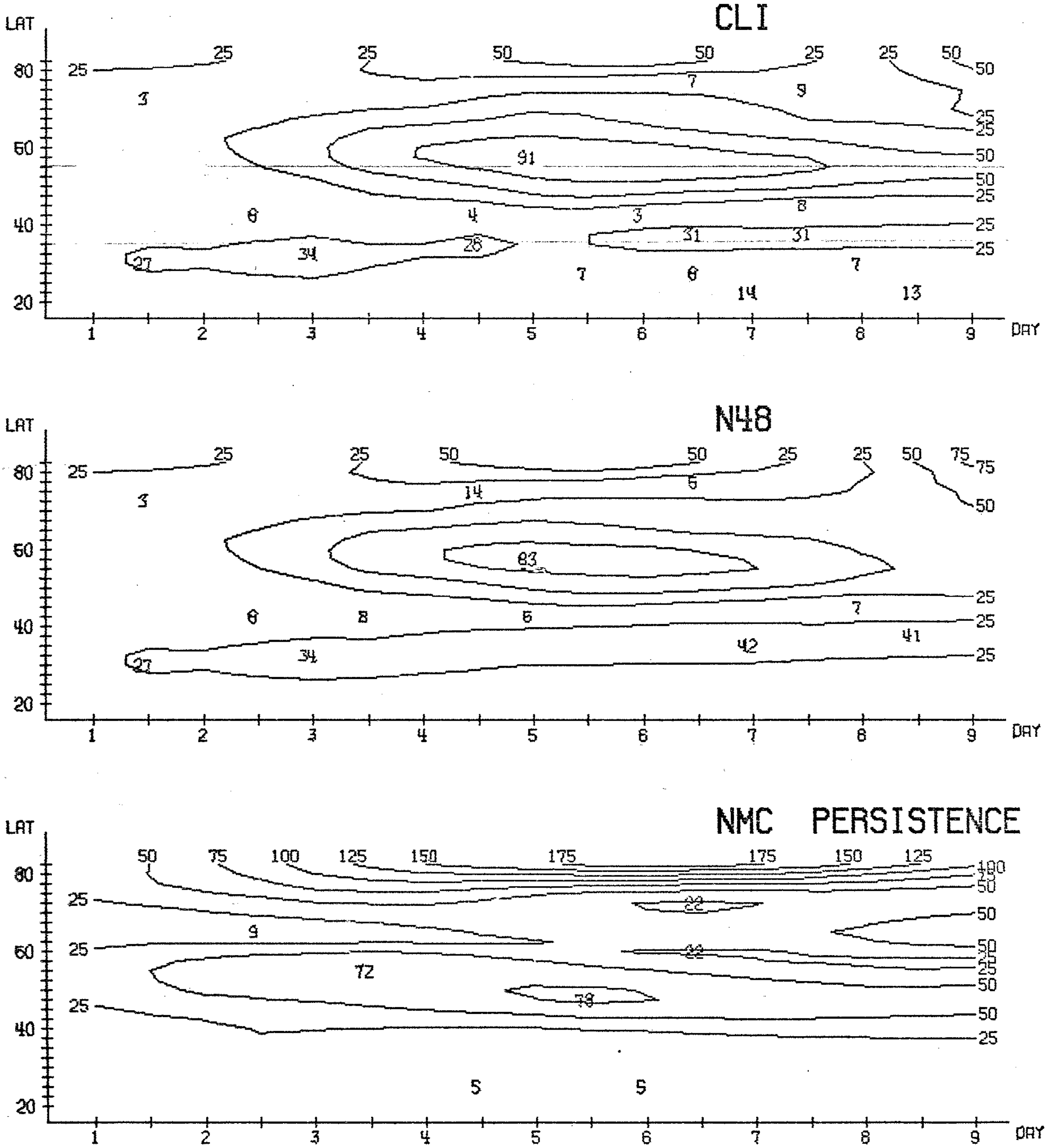

ZONAL PART MEAN BETWEEN 1000 TO 200 MB
RMS ERROR OF HEIGHT (M) 60 HOUR MEAN

FIGURE 18

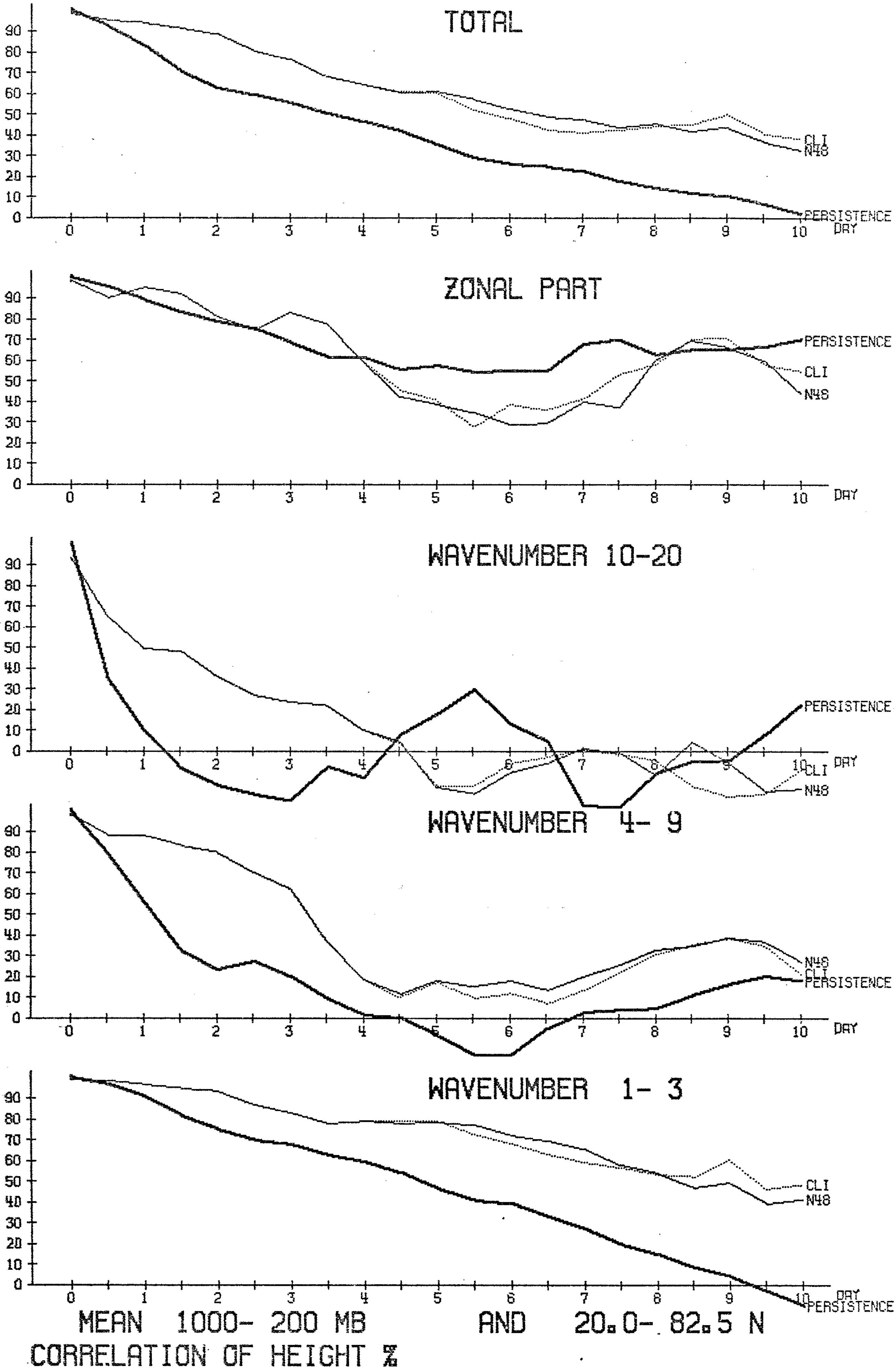
TOTAL
CLI
N48
PERSISTENCE
DAY
ZONAL PART
PERSISTENCE
CLI
N48
DAY
WAVENUMBER 10-20
PERSISTENCE
CLI
N48
DAY
WAVENUMBER 4- 9
N48
CLI
PERSISTENCE
DAY
WAVENUMBER 1- 3
CLI
N48
DAY
PERSISTENCE
MEAN 1000- 200 MB AND 20.0- 82.5 N
CORRELATION OF HEIGHT %

FIGURE 19

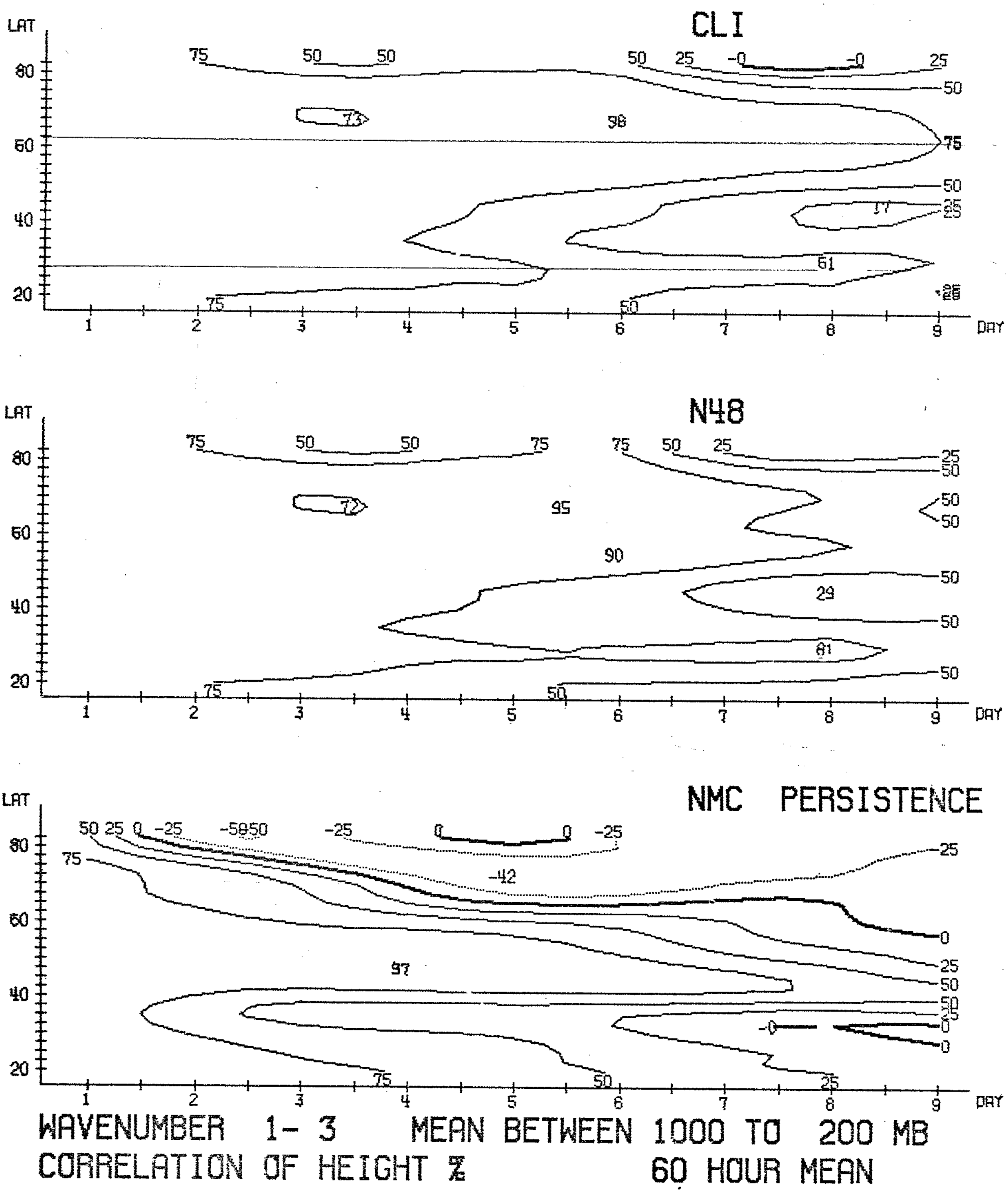
CLI
N48
NMC PERSISTENCE
LAT
DAY
WAVENUMBER 1- 3 MEAN BETWEEN 1000 TO 200 MB
CORRELATION OF HEIGHT % 60 HOUR MEAN

FIGURE 20

3.4 Energetics

For an overview, an integral of kinetic energy over the troposphere north of 20^{o}N is shown in fig. 21. The CLI-run has some better features than the N48-run; that is, more energy for the long and short waves and less energy for the medium waves at the 10th day. The greater kinetic energy in the long waves is mainly due to an increase at higher levels north of 40^{o}N (fig. 22).

The available potential energy in fig. 23 shows a higher similarity with observation for the CLI-run than for the N48-run at the end of the forecast period. The latitudinal variation of the differences for the medium waves are presented in fig. 24. The maximum on the 9th day was forecast too strong by the N48-run and its position was forecast 5^{o} too far north by both runs.

3.5 Results of other experiments in relation to ours

To show how far the results of the above cited experiments differ from ours, in fig. 25 the RMS discrepancies of temperature for the experiment by us and by MIYAKODA and UMSCHEID (1973) are shown. The used models are basically the same but our version had a double as high resolution. Taking the experience by BAUMHEFNER (1972) into account this would mean that our experiment should give greater RMS differences. Also the different averaging area should tend to increase the RMS difference of our experiment. As fig. 25 shows just the opposite, only two reasons are left to explain the advantage of our run.

1.) An imposition of a wall at the equator (as done by MIYAKODA and UMSCHEID) has a much more serious effect on the forecast than taking smooth climatological fields at the southern hemisphere, which is in accordance with DALEY (1974) provided the long waves in the initial data are close to their climatological state.

2.) The fact that the present experiment is for a March case rather than December may be very significant as there is normally a much stronger cross-equatorial flow in Winter than in Spring (see NEWELL,KIDSON, VINCENT and BOER,1972).

It cannot be decided yet which of both reasons is the dominant one.

A comparison with the results of BAUMHEFNER (1971 and 1972) is made in fig. 26. It is likely more difficult to compare these results because the models used are quite different. Our experiment has axisymmetric standing waves of 1 mb amplitude, moving air masses to and fro between both hemispheres which had a very strong influence on the surface pressure and which can be recognised in fig. 26 as oscillations from day 4½ to day 6 . When comparing these results one has to keep in mind that the different seasons and different averaging areas are favouring smaller RMS discrepancies of our model and the different horizontal resolution are favouring the results of BAUMHEFNER (1971).

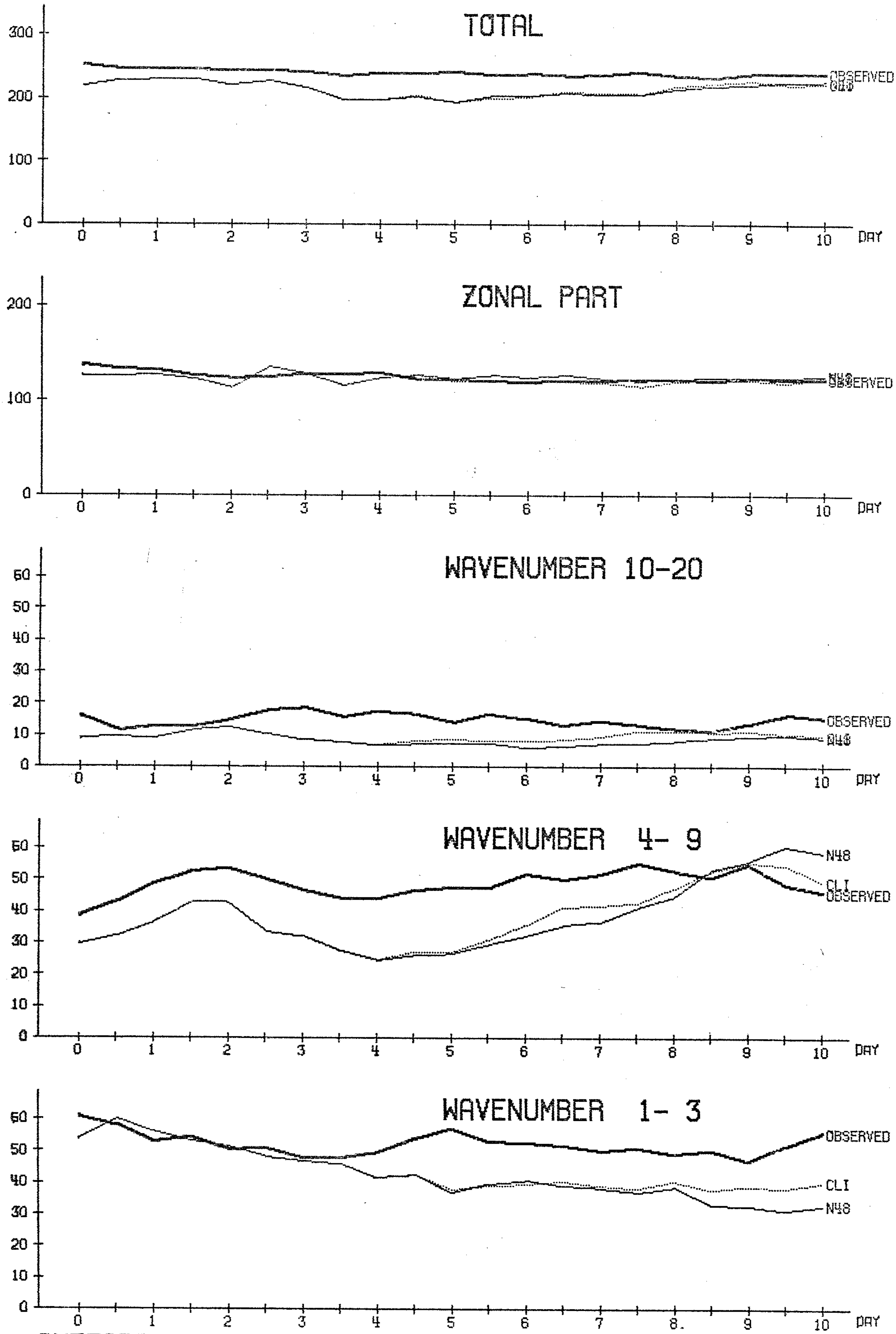

INTEGRAL 1000- 200 MB AREA MEAN 20.0- 82.5 N
KE (10 KJ/M2)

FIGURE 21

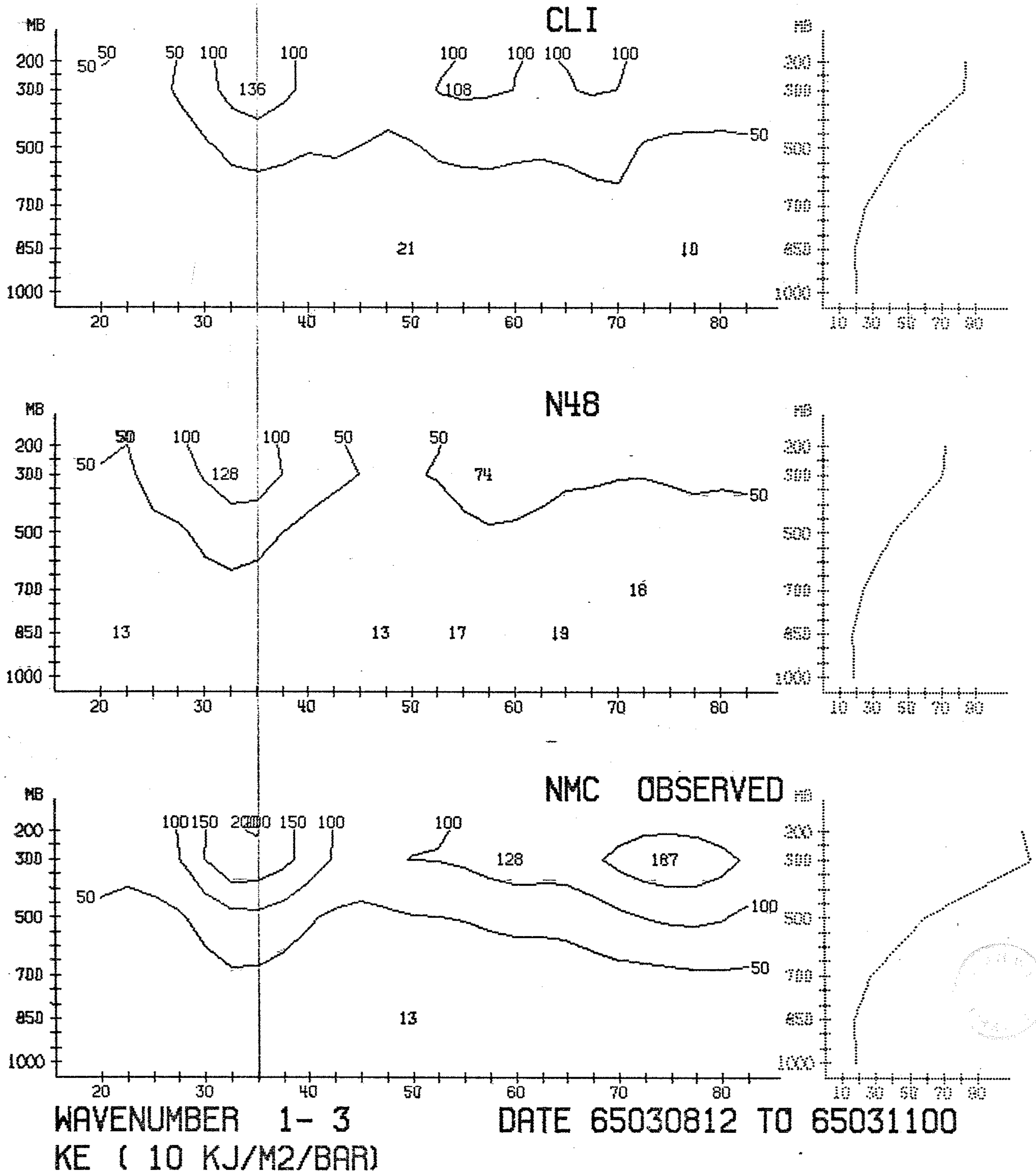
CLI
N48
NMC OBSERVED
MB
200
300
500
700
850
1000
20 30 40 50 60 70 80
10 30 50 70 90
WAVENUMBER 1- 3
DATE 65030812 TO 65031100
KE (10 KJ/M2/BAR)

FIGURE 22

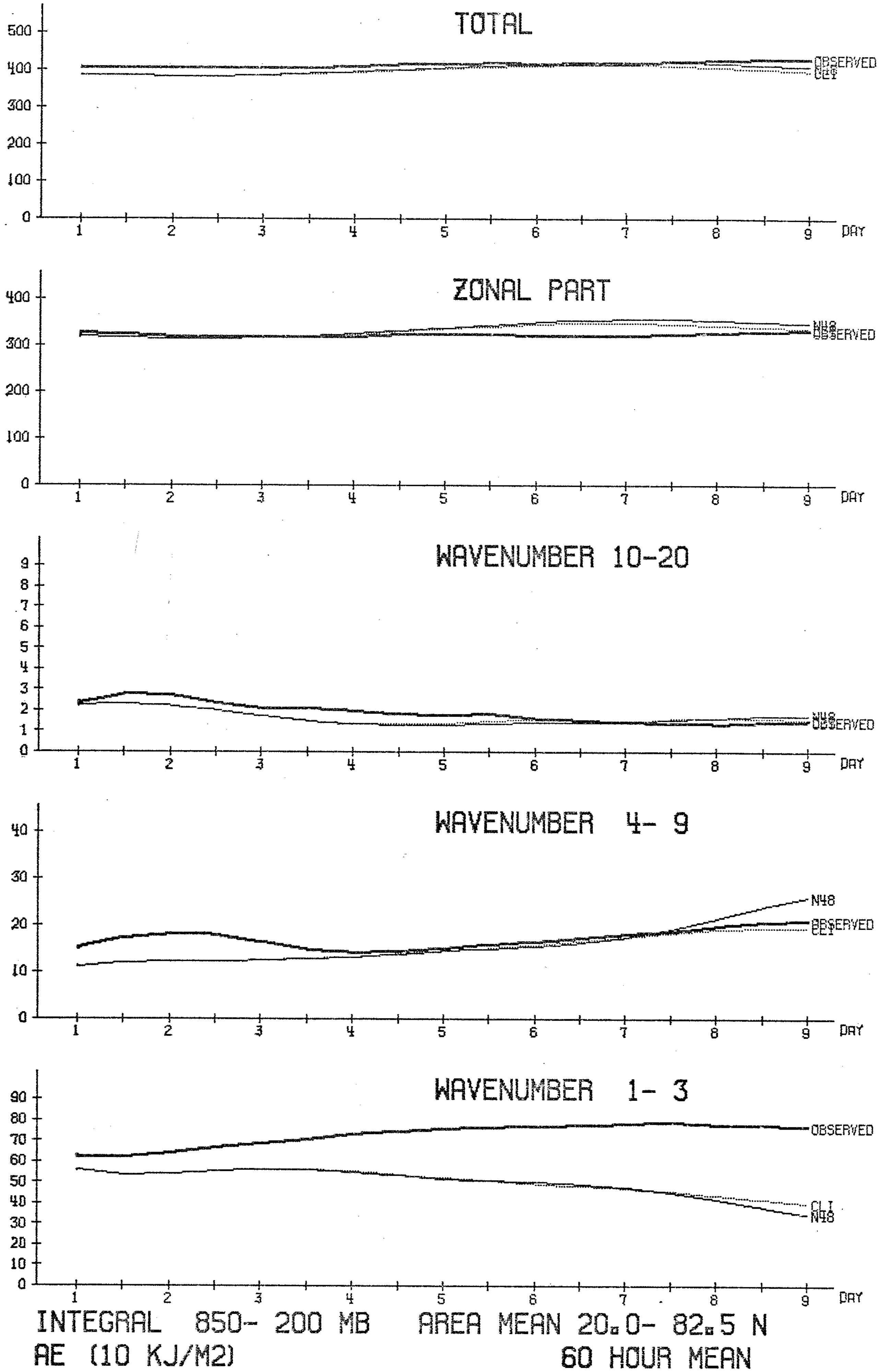
TOTAL
500
400
300
200
100
0
1
2
3
4
5
6
7
8
9
DAY
OBSERVED
N48
CLI
ZONAL PART
400
300
200
100
0
N48
OBSERVED
WAVENUMBER 10-20
9
8
7
6
5
4
3
2
1
0
N48
OBSERVED
WAVENUMBER 4- 9
40
30
20
10
0
N48
OBSERVED
CLI
WAVENUMBER 1- 3
90
80
70
60
50
40
30
20
10
0
OBSERVED
CLI
N48
INTEGRAL 850- 200 MB AREA MEAN 20.0- 82.5 N
AE (10 KJ/M2) 60 HOUR MEAN

FIGURE 23

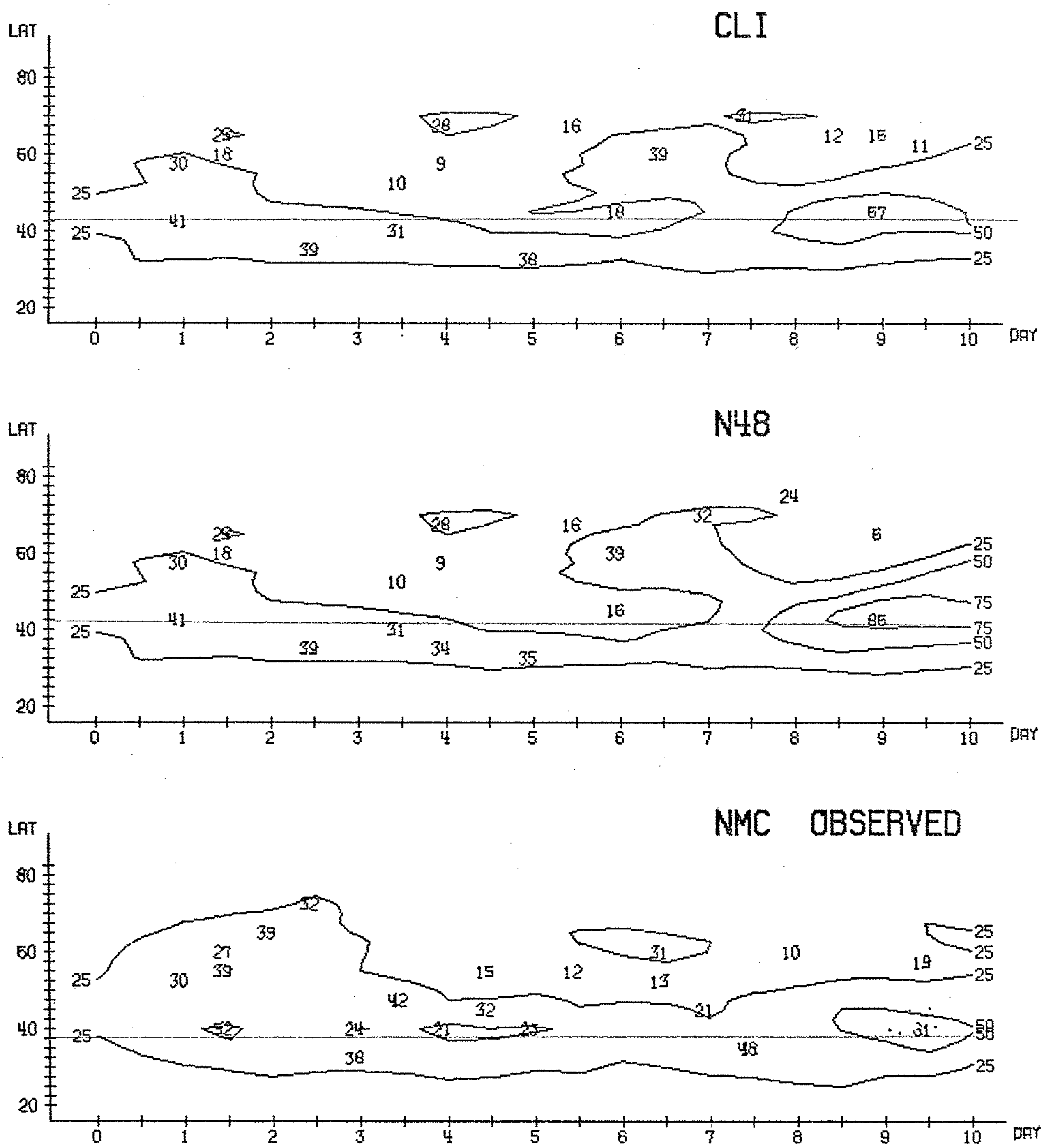

WAVENUMBER 4- 9 INTEGRAL FROM 850 - 200 MB
AE (10 KJ/M2)

FIGURE 24

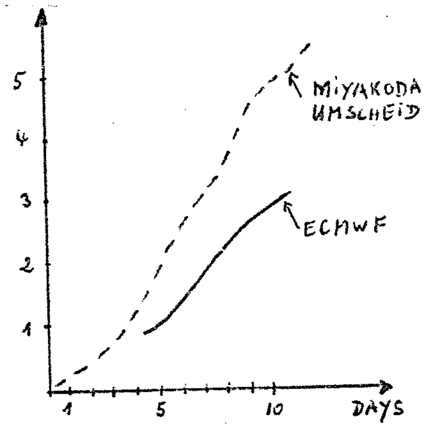

FIGURE 25:

RMS discrepancies of temperature between control runs ar
the experiment imposing a wall at the equator
(MIYAKODA and UMSCHEID) or the experiment replacing
southern hemispheric analyses by climatology (ECMWF).

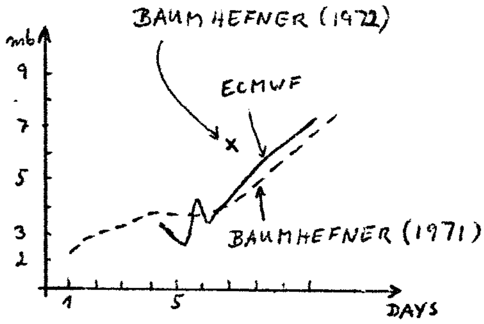

FIGURE 26:

RMS discrepancies of surface pressure
between control runs and the experiment imposing
a wall at the equator (BAUMHEFNER,1971 and 1972)
or the experiment replacing southern hemispheric
analyses by climatology (ECMWF). BAUMHEFNER used
two different resolutions : 5° (1971) and
2.5° (1972).

4. Summary and Conclusions

This comparison between two forecasts, one using global analyses as initial data and one using only the northern hemispheric part of these analyses and climatology for the southern hemisphere, was done to see the influence on the quality of forecasts when southern hemispheric data are replaced by smooth climatological fields. On the whole, both forecasts looked much more similar to each other than to observation. It was surprising that in cases of discrepancies between the two the forecast based on southern hemispheric climatology seemed better in many respects.

Two conclusions out of this are possible.

1.) The effects of the southern hemisphere on the northern hemisphere within 10-day forecasts are small.

2.) The forecasts based on initial analyses of the southern hemisphere were worse than those based on climatology in some important resepcts (e.g. the long waves).

We should remember however that it was just one case which happened to give such results.

As results of similar investigations agree with our results in many respects conclusion 1) is most likely. Even before the Centre's forecast model becomes available we should do another experiment of this kind for a date when a maximum interaction between both hemispheres is expected. Another point which should be investigated is the fact that by spectral decomposition, a growth of non-correlation from the north pole could be seen which was not found in the total fields.

References:

Arpe, K., Bengtsson, L., Hollingsworth, A. and Janjic, Z. (1976) A Case Study of a Ten Day Prediction. ECMWF Technical Report No. 1,105 p.

Baumhefner, D.P. (1971) On the effects of an imposed southern boundary on numerical weather prediction in the northern hemisphere. J. Atm. Sci. 28, 42-54.

Baumhefner, D.P. (1972) Further experimentation with an imposed southern boundary for large-scale numerical weather prediction . J. Atm. Sci., 29, 768-772.

Daley, R. (1974) Cross-equatorial error propagation A numerical simulation. Atmosphere, 12, 125-132.

Jenne, R.L., Crutcher, H.L. van Loon, H. and J.J. Taljaard (1974) A selected climatology of the southern hemisphere : Computer methods and data availability NCAR-TN/STR-92, 91 p. Data on magnetic tape.

Miyakoda, K., Strickler, R.F. and Hembree, G.D. (1970) Numerical Simulation of the Breakdown of a Polar-Night-Vortex : the Stratosphere. Journal of Atm.Sci., 27, 139-154.

Miyakoda, K. Moyer, R.W., Stambler,H., Clarke, R.H. and Strickler, R.F. (1971) A Prediction Experiment with a Global Model on the Kurihara Grid. Journal of Met. Soc. of Japan, 49. 521 - 536.

Miyakoda, K. and L.Umscheid (1973) Effects of an Equatorial "Wall" on an Atmospheric Model. Mon. Wea. Rev. 101, 603-616.

Miyakoda, K. Sadler, J.C. and Hembree, G.D. (1974) An Experimental Prediction of the Tropical Atmosphere for the Case of March 1965. Mon. Wea. Rev. 102/8, 571-591.

Newell, R.E., Kidson, J.W., Vincent, D.G. and Boer, G.J. (1972) The General Circulation of the Tropical Atmosphere. MIT-Press. Vol. I.

Smagorinsky, J., Miyakoda, K. and R.F. Strickler (1970) The relative importance of variabl in initial conditions for dynamical weather prediction. Tellus, 22, 141 - 157.

EUROPEAN CENTRE FOR
MEDIUM RANGE WEATHER
FORECASTS

Research Department (RD)

Internal Report No. 2

ECMWF LIBRARY